

## **Mathematical modelling of the spatio-temporal response of cytotoxic T-lymphocytes to a solid tumour**

ANASTASIOS MATZAVINOS<sup>†</sup> AND MARK A. J. CHAPLAIN<sup>‡\*</sup>

*The SIMBIOS Centre, Division of Mathematics, University of Dundee,  
Dundee, DD1 4HN, UK*

AND

VLADIMIR A. KUZNETSOV<sup>§</sup>

*Laboratory of Integrative and Medical Biophysics, National Institute of Child Health  
& Human Development, National Institutes of Health, Bethesda, MD 20892, USA*

[Received on 9 April 2003; revised on 23 September 2003]

In this paper a mathematical model describing the growth of a solid tumour in the presence of an immune system response is presented. In particular, attention is focused upon the attack of tumour cells by so-called tumour-infiltrating cytotoxic lymphocytes (TICLs), in a small, multicellular tumour, without necrosis and at some stage prior to (tumour-induced) angiogenesis. At this stage the immune cells and the tumour cells are considered to be in a state of dynamic equilibrium—cancer dormancy—a phenomenon which has been observed in primary tumours, micrometastases and residual disease after ablation of the primary tumour. Nonetheless, the precise biochemical and cellular mechanisms by which TICLs control cancer dormancy are still poorly understood from a biological and immunological point of view. Therefore we focus on the analysis of the spatio-temporal dynamics of tumour cells, immune cells and chemokines in an immunogenic tumour. The lymphocytes are assumed to migrate into the growing solid tumour and interact with the tumour cells in such a way that lymphocyte-tumour cell complexes are formed. These complexes result in either the death of the tumour cells (the normal situation) or the inactivation (sometimes even the death) of the lymphocytes. The migration of the TICLs is determined by a combination of random motility and chemotaxis in response to the presence of chemokines. The resulting system of four nonlinear partial differential equations (TICLs, tumour cells, complexes and chemokines) is analysed and numerical simulations are presented. We consider two different tumour geometries—multi-layered cell growth and multi-cellular spheroid growth. The numerical simulations demonstrate the existence of cell distributions that are quasi-stationary in time and heterogeneous in space. A linear stability analysis of the underlying (spatially homogeneous) ordinary differential equation (ODE) kinetics coupled with a numerical investigation of the ODE system reveals the existence of a stable limit cycle. This is verified further when a subsequent bifurcation analysis is undertaken using a numerical continuation package. These results then explain the complex heterogeneous spatio-temporal dynamics observed in the partial differential equation (PDE) system. Our approach may lead to a deeper understanding of

<sup>†</sup>Email: [tasos@maths.dundee.ac.uk](mailto:tasos@maths.dundee.ac.uk)

<sup>‡</sup>Email: [chaplain@maths.dundee.ac.uk](mailto:chaplain@maths.dundee.ac.uk)

<sup>§</sup>Email: [vk28u@nih.gov](mailto:vk28u@nih.gov)

\*To whom reprint requests should be sent

the phenomenon of cancer dormancy and may be helpful in the future development of more effective anti-cancer vaccines.

*Keywords:* solid tumour growth; immune response; T-lymphocytes; chemokines; spatio-temporal heterogeneity.

## 1. Introduction

A neoplasm (solid tumour) may be defined as ‘... *an abnormal mass of tissue whose growth exceeds that of normal tissue, is un-coordinated with that of the normal tissue, and persists in the same excessive manner after cessation of the stimuli which evoked the change.*’ (MacSween & Whaley, 1992). A cancer, or malignant tumour, is a tumour that invades surrounding tissues, traverses at least one basement membrane zone, grows in the mesenchyme at the primary site and has the ability to grow in a distant mesenchyme, forming secondary cancers or metastases. It has been widely proposed that tumours which originate spontaneously in humans or animals often grow slowly or exist for a long period of time in a near-steady-state size even when tumour cells express activated oncogenes or enhanced growth factor signalling mechanisms. Many months, years, or even dozens of years may be required for the clinical manifestation of cancers (Siu *et al.*, 1986; Uhr *et al.*, 1991; Wheelock *et al.*, 1981; Lord & Nardella, 1980). A solid tumour which is ‘near-steady-state’ is described by the term *cancer dormancy* (Alsabti, 1978; Wheelock *et al.*, 1981). The tumour nodule grows to an approximate size of 1–3 mm in diameter, containing around  $10^5 - 10^6$  cells and then growth slows down and sometimes ceases. However, there are well documented clinical observations of ‘latent’ or ‘dormant’ human tumours containing  $10^9$  cells or even more (Bohman, 1976; Alsabti, 1978; Wheelock *et al.*, 1981). Recent studies of the early steps in metastasis (the spread of secondary tumours) have suggested that solitary cancer cells that are neither proliferating nor undergoing apoptosis in sufficiently large numbers could contribute to metastatic recurrence after a period of ‘clinical dormancy’ (Naumov *et al.*, 2002). Cancer dormancy is often observed in breast cancer, neuroblastoma, melanoma, osteogenic sarcoma, and in several types of lymphomas, and is often found ‘accidentally’ in tissue samples of healthy individuals who have died suddenly (Breslow *et al.*, 1977; Alsabti, 1978). In some cases, cancer dormancy has been found in cancer patients after several years of front-line therapy and clinical remission. The presence of these cancer cells in the body determines, finally, the outcome of the disease. In particular, age, stress factors, infections, act of treatment itself or other alterations in the host can provoke the initiation of uncontrolled growth of initially dormant cancer cells and waves of metastases (Uhr & Marches, 2001; Holmberg & Baum, 1996).

Recently, some molecular targets for the induction of cancer dormancy and the re-growth of a dormant tumour have been identified (Aguirre Ghiso, 2002; Udagawa *et al.*, 2002). However, the precise nature of the phenomenon remains poorly understood.

The early stage of primary tumour formation often occurs in the absence of a vascular network. According to Folkman (1985) and Retsky *et al.* (1987), this stage may last up to several years. This limitation of growth is attributed by researchers to the competition between tumour cells for metabolites, direct cytostatic/cytotoxic effect produced by the tumour cells on each other, and the competition between tumour cells and cells of the

immune system for metabolites. In some cases in solid tumours there is a balance between cell proliferation and cell death. This steady-state of a fully malignant tumour (i.e. with the potential for invasion and metastases), but one which is under the local control of the host (e.g. via the immune system, endocrine system, contact inhibition), could persist for months or years (Uhr & Marches, 2001).

One of the reasons for the slow growth of tumours and, in some cases, for their regression, may be the reaction of the host immune system to the nascent tumour cells. It has been demonstrated that tumour-associated antigens could be expressed on tumour cells at very early stages of tumour progression. Such changes are sufficient for intensive lymphoid, granulocyte and monocyte infiltration of a tumour. Especially pronounced infiltration may correlate with a favourable prognosis (Brocker *et al.*, 1988; Lord & Nardella, 1980; Lord & Burkhardt, 1984). The early (avascular) stage and the subsequent stages of tumour growth are characterized by a chronic inflammatory infiltration of neutrophils, eosinophils, basophils, monocytes/macrophages, T-lymphocytes, B-lymphocytes and natural killer (NK) cells (Lord & Nardella, 1980; Sordat *et al.*, 1980; Wilson & Lord, 1987). These cells penetrate the interior of the tumour and accumulate in it due to attractants secreted from the tumour tissue and the high locomotive ability of activated immune cells (Ratner & Heppner, 1986). Indeed during the avascular stage, tumour development can be effectively eliminated by *tumour-infiltrating cytotoxic lymphocytes (TICLs)* (Loeffler & Ratner, 1989). The TICLs may be cytotoxic lymphocytes (CTLs, CD8<sup>+</sup> cells), natural killer-like (NK-like) cells and/or lymphokine activated killer (LAK) cells (Deweger *et al.*, 1987; Forni *et al.*, 1994; Lord & Burkhardt, 1984; Wilson & Lord, 1987). Cytostatic/cytotoxic activity of granulocytes and monocytes/macrophages located in the tumour is found less frequently (Deweger *et al.*, 1987; Forni *et al.*, 1994; Suzuki *et al.*, 1987).

An important factor, which may influence the outcome of the interactions between tumour cells and TICLs in a solid tumour, is the spatial distribution of the TICLs. A thick shell of lymphoid infiltration is often revealed around the tumour (Berezhnaya *et al.*, 1986; Clark, 1991) and even near the central hypoxic zone (Loeffler *et al.*, 1988). This would define an internal structure, whereby the regions of cell proliferation and cell death alternate, with the TICLs located near the groups of dying tumour cells (Nesvetov & Zhdanov, 1981).

In spite of some progress into the investigation of TICLs and their mechanisms of interaction with tumour cells, our understanding of the spatio-temporal dynamics of TICLs in avascular tumours and in micrometastases *in vivo* is still rather limited. It is perhaps not surprising therefore, that this complicated picture has not yet received an adequate explanation. Certainly, other components of the immune system (e.g. cytokines) are involved in modulating the local cellular immune response dynamics. Production of several interleukins (IL-2, IL-10, IL-12) cell-adhesion molecules (i.e. ICAM-1) and chemokines (i.e. LEC) in tumour tissue induce chemotaxis of T-cells and cytotoxic reactions of TICLs against tumour cells (Friedl *et al.*, 1995; Giovarelli *et al.*, 2000; Cairns *et al.*, 2001). Many cytokines are produced during cell-cell interactions, which can be focused to perform their function over short ranges in space and over short intervals of time. Strong local immune reactions are induced by the release of many interleukins, G-CSF, interferons, and tumour necrosis factors. These cytokines are known to recruit and activate a variety of cell types (often in different ways), which could be tumour-infiltrating cells, or the tumour

cells themselves (Forni *et al.*, 1994; Puri & Siegel, 1993; Schwartzenruber *et al.*, 1991; Kuznetsov & Puri, 1999). Besides effector immune reactions, other processes (e.g. cell proliferation, development, locomotion and apoptosis) are governed in a feedback fashion by their own intensity.

Over the last 20 years three-dimensional tissue cultures have been increasingly used to model the heterogeneity of micro-environmental and population changes which develop in solid tumours. There are two geometrically different experimental models—multicellular tumour spheroids (Sutherland, 1988) and multi-layered cell tissue (Cowan *et al.*, 1996). Both of these experimental systems mimic the tumour environment better than mono-layer cell cultures because their spatial structure permits more cell–cell interactions and also permits the modelling of physical constraints. Numerous studies have been undertaken to examine the different mechanisms of migration and infiltration of immune cells and their interactions with the tumour cell populations within such tumour models (Lord & Nardella, 1980; Friedl *et al.*, 1995; Jaaskelainen *et al.*, 1992). However the effect of the immune cells on the tumour cells has been mainly evaluated only crudely by the survival of the tumours without a detailed spatio-temporal analysis of processes in the tumour. One obstacle to the interpretation and analysis of data obtained from such experiments is a lack of a quantitative methodology for the characterization both of the spatio-temporal patterns of the distributions in these experimental systems, and also of the large variations at the cell level between different tumour cell types and different populations of immune cells (these differences remarkably affect the efficiency of the immune control of tumour growth).

It is difficult to control experimentally all of the interacting elements in a tumour. Furthermore, complex biological systems, such as the immune system and a cancer *in vivo*, do not always behave or act as predicted by experimental investigations *in vitro* (Prehn, 1994). It has been shown that mathematical modelling and computer simulations can be helpful in understanding some important features in these elaborate systems (Kuznetsov, 1992; Adam, 1993; Adam & Bellomo, 1997).

In recent years several papers have begun to investigate the mathematical modelling of various aspects of the spatial features associated with the immune response to cancer. Specific aspects include lymphocyte diffusion, proliferation and cell–cell interactions in solid tumours (Kuznetsov, 1992; Kuznetsov & Stepanova, 1992; Chaplain *et al.*, 1998), tumour cell and macrophage interactions (Byrne & Owen, 2001; Owen & Sherratt, 1997, 1998; Kelly *et al.*, 2002; Owen & Sherratt, 1999; Sherratt *et al.*, 1999) and receptor–ligand dynamics (Fas–FasL) (Webb *et al.*, 2002). Numerical and bifurcation analysis of these models have demonstrated diverse patterns of spatio-temporal dynamics of the immune and tumour cells within tumour tissue, even in dormant tumours which are being controlled by cytotoxic lymphocytes.

In this paper, a mathematical model describing the spatio-temporal dynamics of a solid tumour *in vivo* under the control of the immune response of TICLs, is presented. We consider two different tumour geometries—multi-layered cell growth (see Section 2) and the multi-cellular spheroid (see Section 6). The model is an extension and development of work in Kuznetsov (1992), Kuznetsov & Stepanova (1992) and Chaplain *et al.* (1998). The complex dynamics of the interactions between immune cells and tumour cells, in a solid tumour, without necrosis and at some stage prior to (tumour-induced) angiogenesis are discussed. The analysis of the model to be presented in this paper demonstrates that the complex behaviour of the system depends critically upon certain key parameters, in

particular, on the probability of immune cell death/inactivation on encountering a tumour cell, on the binding rate of the immune cells with cancer cells as well as on the chemotactic response of the immune cells to the presence of specialized attraction factors called chemokines.

The layout of the paper is as follows: in the next section we introduce and describe the mathematical model. In Section 3 we present the results of numerical simulations of our model. In Section 4 we undertake a linear stability analysis of the underlying reaction kinetics and a numerical investigation of the phase space dynamics. In Section 5 we undertake a bifurcation analysis of our ODE system using the numerical continuation package XPPAUT. In Section 6 we consider our model in a radially symmetric ‘three dimensional’ geometry. Finally in Section 7 concluding remarks are made.

## 2. The mathematical model

Let us consider a simplified process of a small, growing, avascular tumour which elicits a response from the host immune system and attracts a population of lymphocytes. The growing tumour is directly attacked by TICLs (Ioannides & Whiteside, 1993; Jaaskelainen *et al.*, 1992; Kawakami *et al.*, 1993) which, in turn, secrete soluble diffusible factors (chemokines). These factors enable the TICLs to respond in a chemotactic manner (in addition to random motility) and migrate towards the tumour cells. Our model will therefore consist of six dependent variables denoted  $E$ ,  $T$ ,  $C$ ,  $E^*$ ,  $T^*$  and  $\alpha$ , which are the local densities/concentrations of TICLs, tumour cells, TICL–tumour cell complexes, inactivated TICLs, ‘lethally hit’ (or ‘programmed-for-lysis’) tumour cells, and a single (generic) chemokine respectively.

We first of all consider the local interactions between the TICLs and tumour cells *in vivo* which may be described by the simplified kinetic scheme given in Fig. 1 (see Kuznetsov, 1991; Kuznetsov *et al.*, 1994 for full details). The parameters  $k_1$ ,  $k_{-1}$  and  $k_2$  are non-negative kinetic constants:  $k_1$  and  $k_{-1}$  describe the rate of binding of TICLs to tumour cells and detachment of TICLs from tumour cells *without* damaging cells;  $k_2$  is the rate of detachment of TICLs from tumour cells, resulting in an irreversible programming of the tumour cells for lysis (i.e. death) with probability  $p$  or inactivating/killing TICLs with probability  $(1 - p)$ . For the first time, the possibility of a direct ‘counterattack’ against the effector immune cells was theoretically postulated by Kuznetsov in his modelling of the local interaction of cytotoxic lymphocytes and tumour cells *in vivo* (Kuznetsov, 1979). Recently, it has been shown that such a mechanism might be realized through the Fas receptor (Fas, Apo-1/CD95) and its ligand (FasL, CD95L) (O’Connell *et al.*, 1999). Engagement of Fas on a target cell by FasL triggers a cascade of cellular events that result in programmed-cell-death. Both these transmembrane proteins (belonging to the tumour necrosis factor (TNF) family of receptors and ligands) are expressed on the surface of immune cells, including T-lymphocytes and NK-cells. However, many non-lymphoid tumour cells also express FasL which can counterattack and kill the Fas-sensitive tumour-infiltrating lymphocytes. On the other hand, most cancer cells, unlike normal cells, are relatively resistant to Fas-mediated apoptosis by the immune cells. Resistance to programmed-cell-death (apoptosis) through the Fas receptor pathway coupled with expression of the Fas ligand might enable many cancer cells to deliver a ‘counterattack’ against attached cytotoxic lymphocytes.

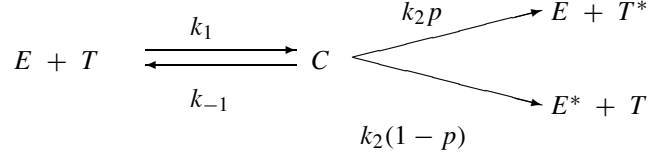


FIG. 1. Schematic diagram of local lymphocyte-cancer cell interactions.

Using the law of mass action, the above kinetic scheme can be ‘translated’ into a system of ordinary differential equations

$$\frac{dE}{dt} = -k_1 ET + (k_{-1} + k_2 p)C, \quad (1)$$

$$\frac{dT}{dt} = -k_1 ET + (k_{-1} + k_2(1-p))C, \quad (2)$$

$$\frac{dC}{dt} = k_1 ET - (k_{-1} + k_2)C, \quad (3)$$

$$\frac{dE^*}{dt} = k_2(1-p)C, \quad (4)$$

$$\frac{dT^*}{dt} = k_2 p C. \quad (5)$$

Next we consider other kinetic interaction terms between the variables and examine migration mechanisms for the TICLs, tumour cells and also consider diffusion of the chemokines. We assume that there is no ‘nonlinear’ migration of cells and no nonlinear diffusion of chemokine i.e. all random motility, chemotaxis and diffusion coefficients are assumed constant.

#### *Tumour-infiltrating cytotoxic lymphocytes*

We assume that the TICLs have an element of random motility and also respond chemotactically to the chemokines. There is a source term modelling the underlying TICL production by the host immune system, a linear decay (death) term and an additional TICL proliferation term in response to the presence of the tumour cells. Combining these assumptions with the local kinetics (derived from Fig. 1) we have the following PDE for

TICLs:

$$\begin{aligned} \frac{\partial E}{\partial t} = & \overbrace{D_1 \nabla^2 E}^{\text{random motility}} - \overbrace{\chi \nabla \cdot (E \nabla \alpha)}^{\text{chemotaxis}} + \overbrace{sh(\mathbf{x})}^{\text{supply}} + \overbrace{\frac{fC}{g+T}}^{\text{proliferation}} \\ & - \overbrace{d_1 E}^{\text{decay}} - \overbrace{k_1 ET + (k_{-1} + k_2 p)C}^{\text{local kinetics}}, \end{aligned} \quad (6)$$

where  $D_1$ ,  $\chi$ ,  $s$ ,  $f$ ,  $g$ ,  $d_1$ ,  $k_1$ ,  $k_{-1}$ ,  $k_2$ ,  $p$  are all positive constants.  $D_1$  is the random motility coefficient of the TICLs and  $\chi$  is the chemotaxis coefficient. The parameter  $s$  represents the ‘normal’ rate of flow of mature lymphocytes into the tissue (non-enhanced by the presence of tumour cells). The function  $h(\mathbf{x})$  is a Heaviside function, which aims to model the existence of a subregion of the domain of interest where initially there are only tumour cells and where lymphocytes do not reside. This region of the domain is penetrated by effector cells subsequently through the processes of diffusion and chemotaxis only (see below for a full discussion regarding this assumption).

The proliferation term  $fC/(g+T)$  has been introduced in Kuznetsov (1991) and represents the experimentally observed enhanced proliferation of TICLs in response to the tumour. This functional form is consistent with a model in which one assumes that the enhanced proliferation of TICLs is due to signals, such as released interleukins, generated by effector cells in tumour cell–TICL complexes. We note that the growth factors that are secreted by lymphocytes in complexes (e.g. IL-2) act mainly in an autocrine fashion. That is to say they act on the cell from which they have been secreted and thus, in our spatial setting, their action can be adequately described by a ‘local’ kinetic term only, without the need to incorporate any additional information concerning diffusivity.

#### *Chemokine concentration*

Chemokines are a super-family of small proteins (8-11kD) secreted primarily by leukocytes characterized by a few conserved cystein motifs. Expression of different cytokines and chemokines in tumour tissue (i.e. via gene delivery or the tumour tissue micro-environment) can induce host responses including infiltration of T-cells capable of rejecting immuno-genic tumours (Lee *et al.*, 2000a). However the production of chemokines in tumour tissue as well as the trafficking of lymphocytes into tumour tissue are dynamic, multi-step processes and currently the precise role of chemokines in tumour growth is still controversial (Bar-Eli, 1999; Satyamoorthy *et al.*, 2002).

We assume that the chemokines are produced when lymphocytes are activated by tumour cell–TICL interactions. Thus we define chemokine production to be proportional to tumour cell–TICL complex density  $C$ . Once produced the chemokines are assumed to diffuse throughout the tissue and to decay in a simple manner with linear decay kinetics. Therefore the PDE for the chemokine concentration is

$$\frac{\partial \alpha}{\partial t} = \overbrace{D_2 \nabla^2 \alpha}^{\text{diffusion}} + \overbrace{k_3 C}^{\text{production}} - \overbrace{d_4 \alpha}^{\text{decay}}, \quad (7)$$

where  $D_2$ ,  $k_3$ ,  $d_4$  are positive parameters.

### Tumour cells

For a simplified description of the spatio-temporal growth of a solid tumour in the very early stages of its development, we will use a basic reaction–diffusion equation. On the kinetic level, the growth dynamics of solid tumours may be described adequately by the logistic equation

$$\frac{dT}{dt} = b_1(1 - b_2T)T, \quad (8)$$

which takes into account a density limitation of growth (Kuznetsov *et al.*, 1994; Marušić *et al.*, 1994a,b). The inclusion of a spatial diffusion term in (8) leads to the well-known Fisher–Kolmogorov equation

$$\frac{\partial T}{\partial t} = D_3 \nabla^2 T + b_1(1 - b_2T)T, \quad (9)$$

which has been used by a number of authors for the modelling of the spatio-temporal evolution of solid tumours (Lefever & Erneux, 1984; Drasdo & Höhme, 2003). In particular, the appropriateness of (9) for modelling tumour growth has been discussed in Drasdo & Höhme (2003), where a lattice-free single-cell model of tumour growth *in situ* has been developed. Within realistic ranges of model parameters, the authors were able to provide a quantitative description of the growth curves in certain experiments. Furthermore, they have approximated the spatio-temporal evolution of their discrete model with a Fisher–Kolmogorov equation.

An alternative approach is to modify the logistic growth kinetics by incorporating terms modelling competition for space between various cell types (Gatenby, 1995, 1996). However, in the framework of our model, we will assume that the TICLs do not compete with the tumour cells for space. This is a reasonable assumption since according to observations (Kyle *et al.*, 1999) the volume of extracellular space in tumours is typically in the range 25–65% of the total volume of cells and hence there is enough space for the migration of lymphocytes within a tumour. Also, tumour cells lack the contact inhibition properties of normal cells and destroy the extracellular matrix. This allows the lymphocytes to migrate into the tumour tissue faster than in normal tissue, which has regular extracellular matrix. Therefore we do not explicitly include a term for space competition between the tumour cells and the lymphocytes and thus a logistic growth term is, we believe, a good first modelling approximation to the tumour growth local kinetics.

We assume that migration of the tumour cells may be described by simple random motility and hence the PDE governing the evolution of the tumour cell density is

$$\frac{\partial T}{\partial t} = \overbrace{D_3 \nabla^2 T}^{\text{random motility}} + \overbrace{b_1(1 - b_2T)T}^{\text{logistic growth}} - \overbrace{k_1 ET + (k_{-1} + k_2(1 - p))C}^{\text{local kinetics}}, \quad (10)$$

where  $D_3$  is the random motility coefficient of the tumour cells,  $b_1, b_2, k_1, k_{-1}, k_2, p$  are positive parameters. The maximal growth rate of the tumour cell population is  $b_1$ , which incorporates both cell multiplication (mitosis) and death. The maximum density of the tumour cells is defined, and is represented by the parameter  $b_2^{-1}$  cf. (Durand & Sutherland, 1984; Prigogine & Lefever, 1980).

### *Tumour cell–TICL complexes*

We assume that there is no diffusion of the complexes, only interactions governed by the local kinetics derived from Fig. 1. The absence of a diffusion term is justified by the fact that formation and dissociation of complexes occurs on a time scale of tens of minutes, whereas the random motility of the tumour cells, for example, occurs on a time scale of tens of hours. Thus, the cell–cell complexes do not have time to move. Therefore the equation for the complexes is given by

$$\frac{\partial C}{\partial t} = \overbrace{k_1 ET - (k_{-1} + k_2)C}^{\text{local kinetics}}. \quad (11)$$

### *Inactivated TICLs and dead tumour cells*

We assume that inactivated and ‘lethally hit’ cells are quickly eliminated from the tissue (for example, by macrophages) and do not substantially influence the immune processes being analysed (a slightly more complicated model might consider the re-introduction of the inactivated TICLs at some later stage). Inactivated cells also do not migrate and therefore we have

$$\frac{\partial E^*}{\partial t} = \overbrace{k_2(1-p)C}^{\text{local kinetics}} - \overbrace{d_2 E^*}^{\text{decay}}, \quad (12)$$

$$\frac{\partial T^*}{\partial t} = \overbrace{k_2 p C}^{\text{local kinetics}} - \overbrace{d_3 T^*}^{\text{decay}}. \quad (13)$$

Therefore the complete system is

$$\begin{aligned} \frac{\partial E}{\partial t} &= D_1 \nabla^2 E - \chi \nabla \cdot (E \nabla \alpha) + sh(\mathbf{x}) + \frac{fC}{g+T} - d_1 E \\ &\quad - k_1 ET + (k_{-1} + k_2 p)C, \end{aligned} \quad (14)$$

$$\frac{\partial \alpha}{\partial t} = D_2 \nabla^2 \alpha + k_3 C - d_4 \alpha, \quad (15)$$

$$\frac{\partial T}{\partial t} = D_3 \nabla^2 T + b_1(1 - b_2 T)T - k_1 ET + (k_{-1} + k_2(1-p))C, \quad (16)$$

$$\frac{\partial C}{\partial t} = k_1 ET - (k_{-1} + k_2)C, \quad (17)$$

$$\frac{\partial E^*}{\partial t} = k_2(1-p)C - d_2 E^*, \quad (18)$$

$$\frac{\partial T^*}{\partial t} = k_2 p C - d_3 T^*. \quad (19)$$

It is easy to see that (18) and (19) are only coupled to the full system through the complexes  $C$  and that neither  $E^*$  nor  $T^*$  have any effect on the variable  $C$ . Thus, for the remainder of this paper, it is sufficient to analyse equations (14)–(17) which essentially dictate the behaviour of the complete system.

For the sake of simplicity, in what follows in this section we will consider the case of one-dimensional tumour growth. Later on, in Section 6, we will present some simulations concerning the case of radially symmetric ‘three-dimensional’ growth.

The Heaviside function  $h(\mathbf{x})$  introduced in (14) models the existence of a subregion of the domain of interest where lymphocytes do not reside and which is penetrated by effector cells through the processes of diffusion and chemotaxis only. For instance, consider the specific case of a tumour that appears below the outer surface of a tissue (e.g. in the basal cell layer of the epidermis) and propagates into deeper levels of the tissue, i.e. invades the dermis (vertical tumour growth). This account could describe a nodular malignant melanoma which has no clinically or histologically evident radial growth phase. Of course, a short radial growth phase presumably does exist but dermal invasion is assumed to occur so rapidly that a preinvasive stage is not apparent (MacSween & Whaley, 1992). Invasive growth is extremely insidious and dangerous, giving rise to metastases or secondary tumours (Clark, 1991; Clark *et al.*, 1986). Considering the host’s immune system response to the invasive tumour growth just described, we should note that intra-epidermal lymphocytes constitute only about 2% of skin-associated lymphocytes (the rest reside in the dermis). Intra-epidermal T cells may express a more restricted set of antigen receptors than do lymphocytes in most extracutaneous tissues. In mice (and some other species), many intra-epidermal lymphocytes are T cells that express an uncommon type of antigen receptor formed by  $\gamma$  and  $\delta$  chains instead of the usual  $\alpha$  and  $\beta$  chains of the antigen receptors of  $CD4^+$  and  $CD8^+$  T cells. This is also true of intra-epithelial lymphocytes in the intestine. Neither the specificity nor the function of this T cell subpopulation is clearly defined (Abbas *et al.*, 2000). Thus, for the purposes of our modelling, we can assume that intra-epidermal lymphocytes are not relevant to the evolution of our system. Therefore, we separate the domain of interest to two subregions, an epidermis-like one and a dermis-like one, by introducing the Heaviside function.

We note here that the one-dimensional version of (14)–(17) does not entirely capture the evolution of a malignant melanoma of the skin, since the actual geometry is more intricate and complicated. However, our purpose here is to investigate the dynamics of the model under discussion in a simple one-dimensional setting, which can give interesting insights. Nevertheless, our setting can be modified towards more realistic geometries.

We define the one-dimensional spatial domain to be the interval  $[0, x_0]$ , and we assume that there are two distinct regions in this interval—one region entirely occupied by tumour cells, the other entirely occupied by the immune cells. We propose that an initial interval of tumour localization is  $[0, l]$ , where  $l = 0.2x_0$ . Therefore the function  $h(x)$  (cf. (14)) is defined as follows:

$$h(x) = \begin{cases} 0, & \text{if } x - l \leq 0, \\ 1, & \text{if } x - l > 0. \end{cases}$$

## 2.1 Boundary and initial conditions

We now close the system by applying appropriate boundary and initial conditions. Zero-flux boundary conditions (BC) are imposed on the variables  $E$ ,  $\alpha$ ,  $T$ , which in our system

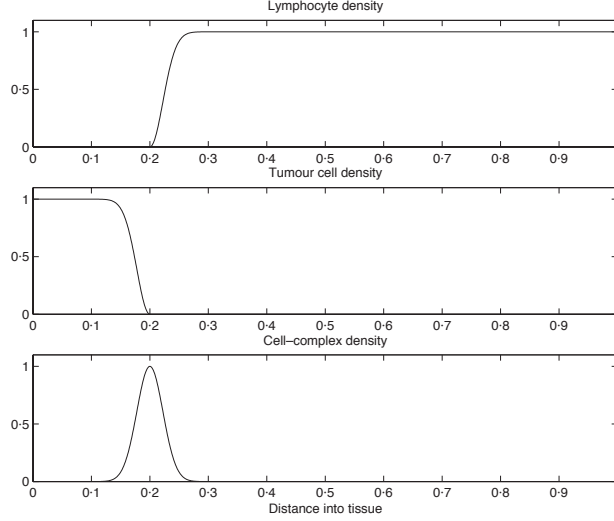


FIG. 2. Initial conditions used for the tumour infiltrating cytotoxic lymphocytes, tumour cells, and complexes.

are equivalent to

$$\mathbf{n} \cdot \nabla E = \mathbf{n} \cdot \nabla \alpha = \mathbf{n} \cdot \nabla T = 0. \quad (20)$$

The initial conditions (IC) are given by

$$\begin{aligned} E(x, 0) &= \begin{cases} 0 & \text{if } 0 \leq x \leq l, \\ E_0(1 - \exp(-1000(x-l)^2)) & \text{if } l < x \leq x_0, \end{cases} \\ T(x, 0) &= \begin{cases} T_0(1 - \exp(-1000(x-l)^2)) & \text{if } 0 \leq x \leq l, \\ 0 & \text{if } l < x \leq x_0, \end{cases} \\ C(x, 0) &= \begin{cases} 0 & \text{if } x \notin [l - \epsilon, l + \epsilon], \\ C_0 \exp(-1000(x-l)^2) & \text{if } x \in [l - \epsilon, l + \epsilon], \end{cases} \\ \alpha(x, 0) &= 0, \forall x \in [0, x_0], \end{aligned} \quad (21)$$

where

$$E_0 = \frac{s}{d_1}, \quad T_0 = \frac{1}{b_2}, \quad C_0 = \min(E_0, T_0), \quad 0 < \epsilon \ll 1.$$

Figure 2 depicts qualitatively the ICs described in (21) (after the non-dimensionalization of the next section), which shows a front of tumour cells encountering a front of TICLs, resulting in the formation of TICL–tumour cell complexes. In the absence of a tumour, the homogeneous steady-state density of the TICLs is  $s/d_1$  and therefore this is the value we have taken for the initial density  $E_0$  of TICLs in the initial conditions. Similarly, in the absence of an immune response, the homogeneous steady-state density of the tumour cells is  $1/b_2$  and this is what we take as the initial density of tumour cells  $T_0$  in

the initial conditions. Thus, when the fronts of the two cell populations meet, the maximum density of TICL–tumour cell complexes will be  $\min(E_0, T_0)$  and hence our choice for  $C_0$ .

## 2.2 Estimation of parameters

In order to carry out an analysis of the model by numerical methods it is useful to estimate values for the parameters obtained from experimental data and work with a non-dimensional system of equations.

The murine B cell lymphoma (BCL<sub>1</sub>) is used as an experimental model of tumour dormancy in mouse (Siu *et al.*, 1986; Uhr & Marches, 2001). It has been demonstrated that CD8<sup>+</sup> T-cells are required for inducing and maintaining dormancy in BCL<sub>1</sub>. In these experiments CD8<sup>+</sup> T cells are enhanced with anti-Id antibodies into inducing dormancy by secreting INF- $\gamma$ . A description of the growth kinetics of a BCL<sub>1</sub> lymphoma in the spleen of recipient mice, chimeric with respect to the Major Histocompatibility Complex (MHC) (Siu *et al.*, 1986), was provided by the model of Kuznetsov *et al.* (1994).

The kinetic parameters (obtained in Chaplain *et al.*, 1998) were determined to have the following values:

$$\begin{aligned} b_1 &= 0.18 \text{ day}^{-1}, & b_2 &= 2.0 \times 10^{-9} \text{ cells}^{-1} \text{cm}, \\ k_1 &= 1.3 \times 10^{-7} \text{ day}^{-1} \text{cells}^{-1} \text{cm}, & k_{-1} &= 24.0 \text{ day}^{-1}, \\ k_2 &= 7.2 \text{ day}^{-1}, & p &= 0.9997, \\ d_1 &= 0.0412 \text{ day}^{-1}, & f &= 0.2988 \times 10^8 \text{ day}^{-1} \text{cells} \cdot \text{cm}^{-1}, \\ g &= 2.02 \times 10^7 \text{ cells} \cdot \text{cm}^{-1}, & s &= 1.36 \times 10^4 \text{ day}^{-1} \text{cells} \cdot \text{cm}^{-1}. \end{aligned}$$

In addition to the kinetic parameters, we require estimates of the cell motility parameters. As we have seen in the previous sections, a tumour may be infiltrated by TICLs as a result of passive migration (random motility) or active transport (chemotaxis). In the first case, the random motility coefficient of the TICLs can be evaluated employing Einstein's formula:

$$D_1 = \frac{kT}{6\pi R_1 \eta},$$

where  $k$  is Boltzmann's constant,  $T$  is the temperature in degrees Kelvin,  $R_1$  is the average radius of a TICL and  $\eta$  is the viscosity coefficient of the medium. With values of  $T = 310 \text{ K}$  ( $37^\circ\text{C}$ ),  $R_1 = 4 \mu\text{m}$  and  $\eta = \eta_{\text{water}}$ , this gives an estimate of the TICL random motility coefficient  $D_1 = 7.0 \times 10^{-5} \text{ cm}^2 \text{ day}^{-1}$ . This value is close to the random motility coefficient of CTLs *in vitro* obtained by Rothstein *et al.* (1978), studying sequential killing of immobilised allogenic tumour cells by CTLs.

The random motility of tumour cells in tissue is conditioned largely by the replication of the cells and the growth of the tumour. The random motility coefficient may therefore be estimated from the following equation (Prigogine & Lefever, 1980):

$$D_3 = 4R_2^2 a,$$

where  $R_2$  is the average radius of a tumour cell and  $a$  is the rate of duplication of the tumour cell population. Assuming  $R_2 = 4 - 15 \mu\text{m}$  and  $a = 0.1 - 1 \text{ day}^{-1}$ , we obtain a range of values  $D_3 = 0.6 - 9 \times 10^{-6} \text{ cm}^2 \text{ day}^{-1}$ .

We know that TICLs are capable of infiltrating solid or lymphoma-like tumours rather rapidly (Jaaskelainen *et al.*, 1992; Lord & Burkhardt, 1984; Ratner & Heppner, 1986; Sordat *et al.*, 1980) and it is apparent that, if the movement of the TICLs and/or tumour cells is an active process induced by chemoattractants, the value of the diffusion coefficients of these cells may be appreciably greater and perhaps even reach approximately  $10^{-2} \text{ cm}^2 \text{ day}^{-1}$  (Friedl *et al.*, 1995; Jaaskelainen *et al.*, 1992). Thus, the intervals of variation of the random motility coefficients may be large, depending upon the physical and biochemical properties of the surrounding tissue matrix and the concentration of various chemoattractants (chemokinesis). However in the simulations to be presented in the subsequent sections we assumed all random motility to be constant and took  $D_1 = D_3 = 10^{-6} \text{ cm}^2 \text{ day}^{-1}$ .

Chemokines diffuse several orders of magnitude faster than cells. A reasonable range of values for the diffusion coefficient of the chemokine  $D_2$  is

$$10^{-4} \text{ cm}^2 \text{ day}^{-1} \leq D_2 \leq 10^{-2} \text{ cm}^2 \text{ day}^{-1}. \quad (22)$$

A more precise estimate for  $D_2$  can be found from the data of Kwok *et al.* (1988), which are concerned with the motion of monoclonal antibodies (MCA). These results can be modified to account for the molecular mass of a typical chemokine (11 kD) and then can be combined with the Stokes–Einstein formula. This yields a value of  $D_2 = 8 \times 10^{-3} \text{ cm}^2 \text{ day}^{-1}$ . However, in our simulations the above range of values for  $D_2$ , given by (22), were used.

The half-life of chemokines is around 60 days (Reisenberger *et al.*, 1996) and so we obtained an estimate for  $d_4$  of  $0.693/60 = 1.155 \times 10^{-2} \text{ day}^{-1}$ . We estimated the chemotactic response of the TICLs from data of macrophages in response to MCP-1 (Sozzani *et al.*, 1991; Owen & Sherratt, 1997). From the range of estimates in these papers we chose a value of  $1.728 \times 10^6 \text{ cm}^2 \text{ day}^{-1} \text{ M}^{-1}$ . The chemokine production parameter  $k_3$  was estimated from data from several groups (Cairns *et al.*, 2001; Murphy & Newsholme, 1999; Lee *et al.*, 2000b). These data estimated the rate of production of chemokine (lymphotactin and IL-8) to be in the range of 20–3000 molecules  $\text{cell}^{-1} \text{ min}^{-1}$ .

Before proceeding with the numerical analysis, we non-dimensionalize our equations in the standard manner.

### 2.3 Non-dimensionalization

We non-dimensionalise (14)–(17), the boundary conditions and initial conditions. An order-of-magnitude density scale is selected for the  $E$ ,  $T$  and  $C$  cell densities, of  $E_0$ ,  $T_0$  and  $C_0$ , respectively, as suggested by the initial conditions. These are then given as  $E_0 \approx 3.3 \times 10^5 \text{ cells} \cdot \text{cm}^{-1}$ ,  $T_0 = 0.5 \times 10^9 \text{ cells} \cdot \text{cm}^{-1}$  and  $C_0 = E_0 \approx 3.3 \times 10^5 \text{ cells} \cdot \text{cm}^{-1}$ .

The chemokine concentration is normalized through some reference concentration  $\alpha_0$  which we take to be  $10^{-10} \text{ M}$  (Nomiya *et al.*, 2001). Time is scaled relative to the diffusion rate of the TICLs, i.e.  $t_0 = x_0^2 D_1^{-1}$ , and the space variable  $x$  is scaled relative to the length of the region under consideration (i.e.  $x_0 = 1 \text{ cm}$ ). Then, on making the following substitutions:

$$\bar{E} = \frac{E}{E_0}, \quad \bar{T} = \frac{T}{T_0}, \quad \bar{C} = \frac{C}{C_0}, \quad \bar{\alpha} = \frac{\alpha}{\alpha_0}, \quad \bar{x} = \frac{x}{x_0}, \quad \bar{t} = \frac{t}{t_0},$$

and omitting the bars for the sake of clarity, (14)–(17) may be re-written as

$$\frac{\partial E}{\partial t} = \nabla^2 E - \gamma \nabla(E \nabla \alpha) + \sigma h(x) + \frac{\rho C}{\eta + T} - \sigma E - \mu ET + \epsilon C, \quad (23)$$

$$\frac{\partial \alpha}{\partial t} = \delta \nabla^2 \alpha + \kappa C - \xi \alpha, \quad (24)$$

$$\frac{\partial T}{\partial t} = \omega \nabla^2 T + \beta_1(1 - \beta_2 T)T - \phi ET + \lambda C, \quad (25)$$

$$\frac{\partial C}{\partial t} = \mu ET - \psi C, \quad (26)$$

where

$$\begin{aligned} \sigma &= \frac{s t_0}{E_0} = d_1 t_0, & \rho &= \frac{f t_0 C_0}{E_0 T_0}, & \mu &= \frac{k_1 t_0 T_0 E_0}{C_0} = k_1 t_0 T_0, \\ \eta &= \frac{g}{T_0}, & \epsilon &= \frac{t_0 C_0 (k_{-1} + k_2 p)}{E_0}, & \omega &= \frac{D_3 t_0}{x_0^2} = D_3 D_1^{-1}, \\ \beta_1 &= b_1 t_0, & \beta_2 &= b_2 T_0, & \phi &= k_1 t_0 E_0, \\ \lambda &= \frac{t_0 C_0 (k_{-1} + k_2 (1-p))}{T_0}, & \psi &= t_0 (k_{-1} + k_2), & \gamma &= \frac{\chi \alpha_0 t_0}{x_0^2} = \chi \alpha_0 D_1^{-1}, \\ \delta &= \frac{D_2 t_0}{x_0^2} = D_2 D_1^{-1}, & \kappa &= \frac{k_3 t_0 C_0}{\alpha_0}, & \xi &= d_4 t_0. \end{aligned}$$

After non-dimensionalization, the boundary conditions become

$$\begin{aligned} \frac{\partial E}{\partial x}(0, t) &= 0, & \frac{\partial E}{\partial x}(1, t) &= 0, \\ \frac{\partial \alpha}{\partial x}(0, t) &= 0, & \frac{\partial \alpha}{\partial x}(1, t) &= 0, \\ \frac{\partial T}{\partial x}(0, t) &= 0, & \frac{\partial T}{\partial x}(1, t) &= 0, \end{aligned}$$

which then imply, assuming some smoothness of the solution and the form of (26),

$$\frac{\partial C}{\partial x}(0, t) = 0, \quad \frac{\partial C}{\partial x}(1, t) = 0.$$

Our initial conditions take the following form:

$$\begin{aligned} E(x, 0) &= \begin{cases} 0 & \text{if } 0 \leq x \leq l, \\ 1 - \exp(-1000(x-l)^2) & \text{if } l < x \leq 1, \end{cases} \\ T(x, 0) &= \begin{cases} 1 - \exp(-1000(x-l)^2) & \text{if } 0 \leq x \leq l, \\ 0 & \text{if } l < x \leq 1, \end{cases} \\ C(x, 0) &= \begin{cases} 0 & \text{if } x \notin [l - \epsilon, l + \epsilon], \\ \exp(-1000(x-l)^2) & \text{if } x \in [l - \epsilon, l + \epsilon], \end{cases} \\ \alpha(x, 0) &= 0, \forall x \in [0, 1]. \end{aligned}$$

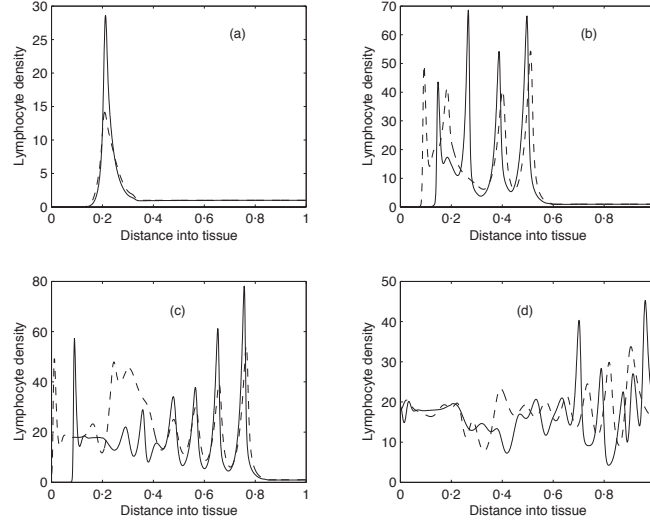


FIG. 3. Spatial distribution of TICL density within the tissue at times corresponding to 100, 400, 700 and 1000 days respectively. Solid line, with chemotaxis; dashed, without (i.e.  $\gamma = 0$ ).

Values for all the non-dimensional parameters are obtained from the estimated dimensional parameters in Section 4. Concerning the chemokine production rate, we note that the data presented in the previous section correspond to *in vitro* experimental settings and that we were unable to find any *in vivo* measurements in the literature. However, it seems reasonable to assume that not all complexes formed *in vivo* result in chemokine production and thus our choice for the value of parameter  $\kappa$  is slightly lower than the minimum value coming from the available *in vitro* data. Therefore, in the following simulations a value of  $\kappa = 10^4$  has been chosen. This value of  $\kappa$  is of the same order of magnitude as that of  $\xi$ , i.e.  $\kappa \approx \xi$ , and we note that this is also in line with the non-dimensional argument presented in Owen & Sherratt (1997).

By employing a numerical method, we obtain solutions for the above non-dimensionalized system, in the following section.

### 3. Numerical simulation results

The non-dimensionalized model was solved numerically using NAG routine D03PCF, which integrates systems of partial differential equations via the method of lines and a stiff ODE solver.

Figures 3(a)–(d) show the spatial distribution of TICL density within the tissue at times corresponding to 100, 400, 700 and 1000 days respectively. The figures show a heterogeneous spatial distribution of TICL density throughout the tissue. Figures 4(a)–(d) show the corresponding spatial distribution of tumour cell density within the tissue at times corresponding to 100, 400, 700 and 1000 days. The figures show a train of solitary-like waves invading the tissue and subsequently creating a spatially heterogeneous distribution of tumour cell density throughout. Figures 5(a)–(d) show the corresponding

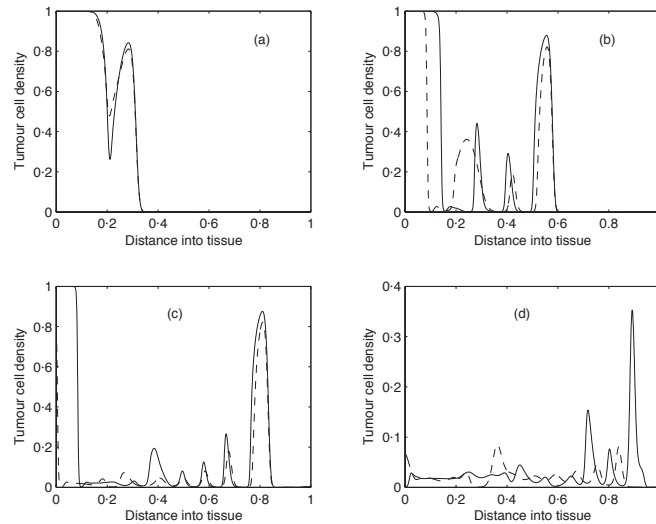


FIG. 4. Spatial distribution of tumour cell density within the tissue at times corresponding to 100, 400, 700 and 1000 days respectively. Solid line, with chemotaxis; dashed, without (i.e.  $\gamma = 0$ ).

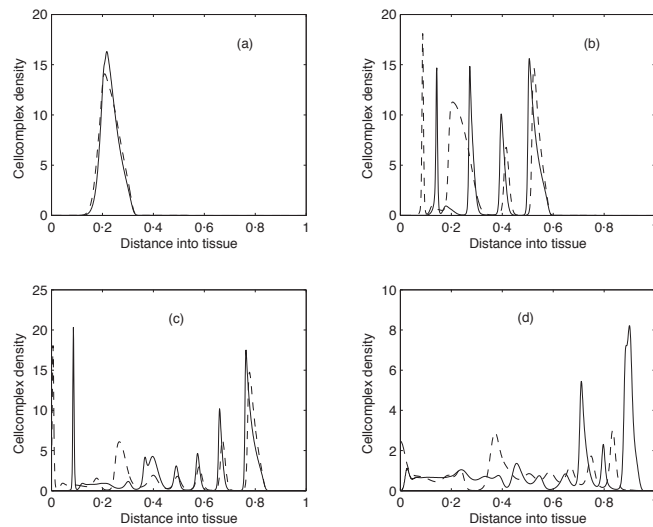


FIG. 5. Spatial distribution of tumour cell-TICL complex density within the tissue at times corresponding to 100, 400, 700 and 1000 days respectively. Solid line, with chemotaxis; dashed, without (i.e.  $\gamma = 0$ ).

spatial distribution of tumour cell-lymphocyte complexes within the tissue at times corresponding to 100, 400, 700 and 1000 days respectively. The dynamics of this spatio-temporal heterogeneity appear to persist as the long-time behaviour of the system in Figs 6–8 shows. The times here correspond to 3000, 5000, 7000 and 10000 days respectively.

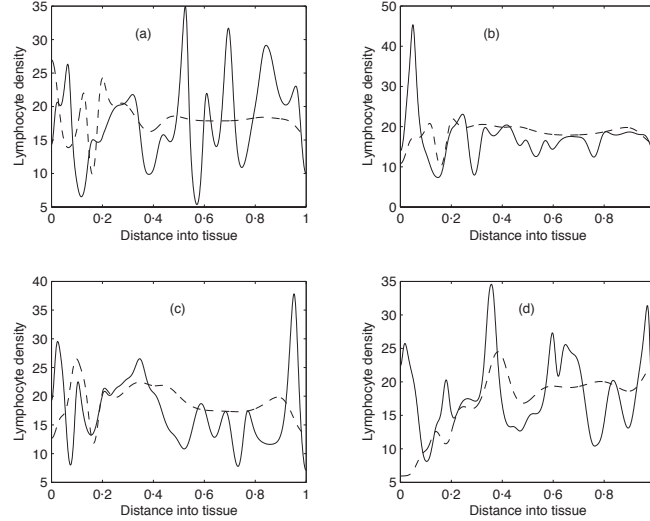


FIG. 6. Spatial distribution of TICL density within the tissue at times corresponding to 3000, 5000, 7000 and 10000 days respectively. Solid line, with chemotaxis; dashed, without (i.e.  $\gamma = 0$ ).

In addition to observing the above spatio-temporal distributions of each cell type within the tissue, the temporal dynamics of the overall populations of each cell type (i.e. total cell number) was examined. This was achieved by calculating the total number of each cell type within the whole tissue space using numerical quadrature. Figure 9(a) shows the variation in the number of TICLs within the tissue over time (approximately 80 years, an estimated average lifespan). Initially, the total number of TICLs within the tissue increases and then subsequently oscillates around some stationary level (approximately  $5.9 \times 10^6$  cells). Long-time numerical calculations indicated that this behaviour will persist for all time.

A similar scenario is observed for the tumour cell population. From Fig. 9(b) we observe that, initially, the tumour cell population decreases in number before subsequently oscillating around some stationary value (approximately  $10^7$  cells) for all time. Figure 9(c) gives the corresponding temporal dynamics of the complexes. Figure 10 provides a more detailed view of the early oscillations in the total number of tumour cells.

The above simulations appear to indicate that eventually the tumour cells develop very small-amplitude oscillations about a ‘dormant’ state, indicating that the TICLs have successfully managed to keep the tumour under control. The numerical simulations demonstrate the existence of cell distributions that are quasi-stationary in time and heterogeneous in space.

Concerning the spatial evolution of cancer dormancy with reference to the aspect of spatial containment, we note that the use of a fixed domain is consistent with various realistic biological settings. BCL<sub>1</sub> lymphomas of the spleen, for instance, are considered to be very good *in vivo* experimental models for investigating the various aspects of tumour development precisely due to the fact that tumour cells are spatially contained within the lymph tissue of the spleen. Spleens in mice are elongated organs with boundaries defined

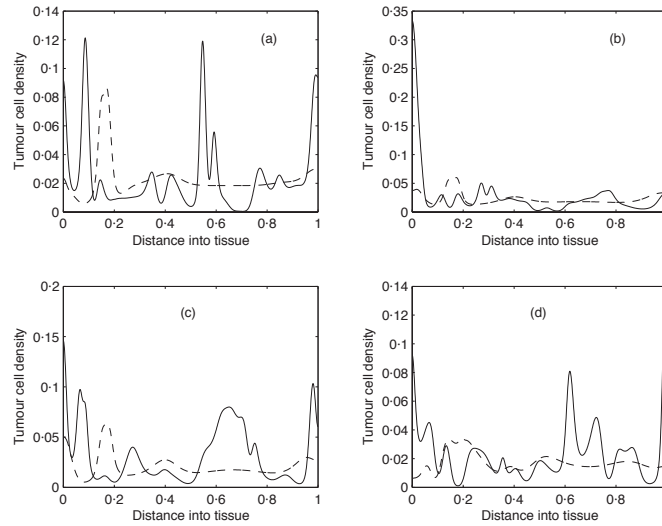


FIG. 7. Spatial distribution of tumour cell density within the tissue at times corresponding to 3000, 5000, 7000 and 10000 days respectively. Solid line, with chemotaxis; dashed, without (i.e.  $\gamma = 0$ ).

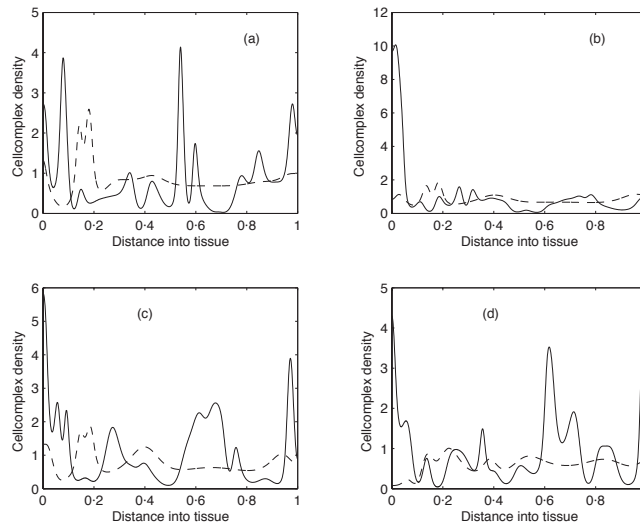


FIG. 8. Spatial distribution of tumour cell-TICL complex density within the tissue at times corresponding to 3000, 5000, 7000 and 10000 days respectively. Solid line, with chemotaxis; dashed, without (i.e.  $\gamma = 0$ ).

by very strong basal membranes, which do not permit the tumour cells to escape unless they break these membranes (through well-known invasive processes) and then initiate metastases. However, in our model, we do not consider these cases and this is why we employ a fixed domain and impose zero-flux boundary conditions. Of course, if the domain

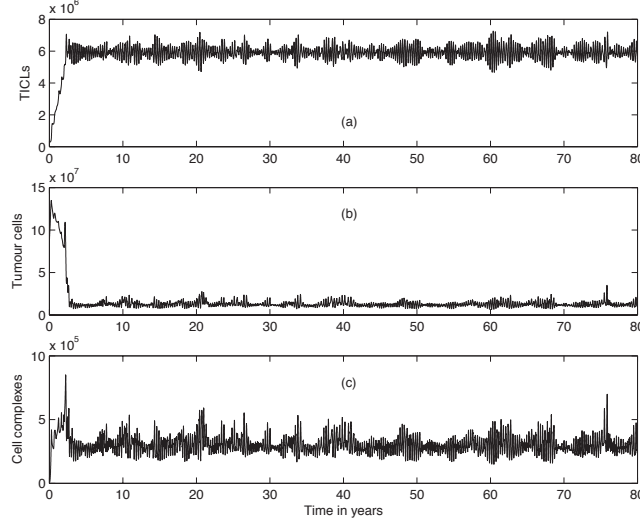


FIG. 9. Total number of (a) lymphocytes, (b) tumour cells, and (c) tumour cell–TICL complexes within tissue over a period of 80 years.

itself were evolving the tumour cells would not be contained in space, but would rather spread throughout the domain. In the latter case we note that, from a mathematical point of view, it would be trivial to induce some kind of spatial containment of the tumour cells in a subregion of the domain by incorporating some non-autonomous ODE kinetics. However, this is not a realistic approach for the biological settings we consider and our numerical simulations do reflect several temporal as well as spatial aspects of tumour dormancy as these are described in various immunomorphological investigations.

The interesting spatio-temporal dynamics of the system (i.e. the irregular invasive ‘waves’) require us to investigate the underlying (spatially homogeneous) kinetics of our system.

#### 4. Linear stability analysis of the spatially homogeneous system

We consider the following autonomous system of ODEs that describes the underlying spatially homogeneous kinetics of (23)–(26) with  $h(x) \equiv 1$ :

$$\frac{dE}{dt} = \sigma + \frac{\rho C}{\eta + T} - \sigma E - \mu ET + \epsilon C, \quad (27)$$

$$\frac{dT}{dt} = \beta_1(1 - \beta_2 T)T - \phi ET + \lambda C, \quad (28)$$

$$\frac{dC}{dt} = \mu ET - \psi C, \quad (29)$$

$$\frac{d\alpha}{dt} = \kappa C - \xi \alpha. \quad (30)$$

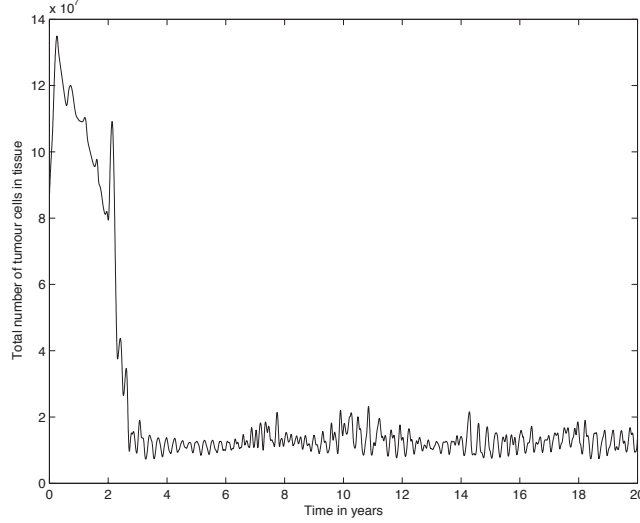


FIG. 10. Total number of tumour cells within tissue over a period of 20 years illustrating the early dynamics. The number of tumour cells initially decreases before settling down to an oscillatory behaviour around a stationary level of approximately  $10^7$  cells.

We note that since, in the above homogeneous system, the chemokine becomes a ‘slave variable’ we will not consider it in the following analysis.

Using the parameter values described in the previous section, it is straightforward to show that there are four steady states of the system (27)–(29) given by

$$\begin{aligned} (E_1, T_1, C_1) &= (1, 0, 0), \\ (E_2, T_2, C_2) &\approx (17.85, 0.02, 0.68), \\ (E_3, T_3, C_3) &\approx (-0.56, 1.03, -1.2), \\ (E_4, T_4, C_4) &\approx (-317, 18.4, -12157). \end{aligned}$$

Obviously  $(E_3, T_3, C_3)$  and  $(E_4, T_4, C_4)$  are biologically unrealistic. Now let  $\mathbf{X}_i = (E - E_i, T - T_i, C - C_i)^T$ ,  $i = 1, 2$ . By linearizing about each steady state  $(E_i, T_i, C_i)$ ,  $i = 1, 2$ , we obtain the following linear system:

$$\frac{d\mathbf{X}_i}{dt} = A_i \mathbf{X}_i$$

where, as usual,  $A_i$  is the Jacobian matrix of the system evaluated at the corresponding steady state.

It is straightforward to show that for  $i = 1$ , there are three real eigenvalues of  $A_i$ , two negative and one positive. Thus,  $(E_1, T_1, C_1)$ , which represents the ‘healthy’ steady state, is unstable. Now for  $i = 2$ , there is only one real eigenvalue of  $A_i$  that is negative, and two complex (conjugate) eigenvalues with positive real part. Thus, the steady state  $(E_2, T_2, C_2)$ , which represents the ‘tumour dormancy’ steady state, is also unstable.

The numerical simulations of the previous section indicated that there are non-standard travelling-wave-like solutions. In order to understand this behaviour we undertook a further

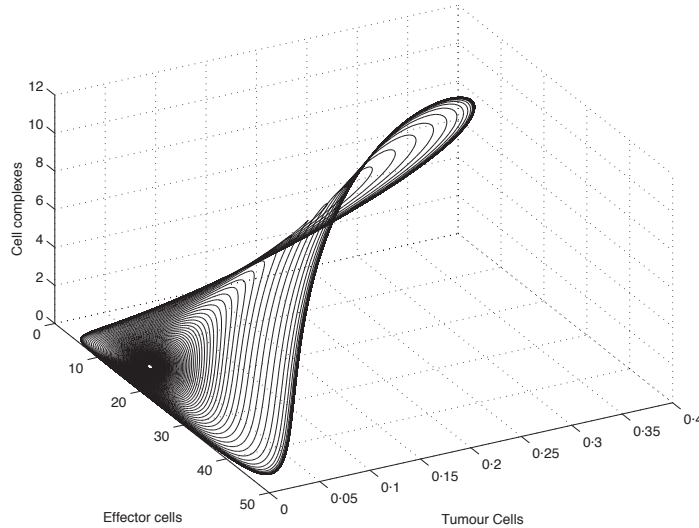


FIG. 11. Orbit of the ODE system with initial conditions near the ‘tumour dormancy’ steady state, converging to the limit cycle.

numerical investigation looking for some additional structure in the  $(E, T, C)$  phase space. The results of numerical computations in this direction are presented in Fig. 11, where the orbit (trajectory) approaches an isolated closed curve in the phase space, i.e. a limit cycle.

It is well reported in the literature that the spatio-temporal behaviour of reaction–diffusion systems with oscillatory kinetics (i.e. kinetics that exhibit a stable limit cycle) can be quite diverse and complicated. An extensive review of such systems can be found in Cross & Hohenberg (1993). In Ermentrout *et al.* (1997) patterns of localized oscillatory regions in reaction–diffusion models for chemical oscillations have been reported. In order for these patterns to appear the kinetics of the PDE systems discussed there must undergo a subcritical Hopf bifurcation and therefore display oscillatory behaviour. We note that we were able to find localized regions of oscillations for a particular choice of initial conditions in our system as well. In Kobayashi *et al.* (1995) the coexistence of a stable stationary solution and a stable limit cycle in a reaction–diffusion model of the Bonhoeffer–van der Pol type has been related to the generation of a self-organized pulse generator and localized oscillatory regions. Also, in Merkin & Sadiq (1996) the behaviour behind invasive wavefronts in a cubic autocatalysis system has been considered. The model presented there undergoes supercritical Hopf bifurcations and is able to depict a wide range of spatio-temporal behaviours, including, under specific conditions, spatio-temporal chaos. Furthermore, the case of spatio-temporal chaos has been investigated in detail in the framework of predator–prey ecological interactions since there exist experimental/field data which seem to corroborate the presence of chaotic behaviour. In particular, reaction–diffusion systems with oscillatory kinetics have been considered in Sherratt *et al.* (1995, 1997). These were able to depict an invasive wave of predators with irregular spatio-temporal oscillations behind the wave front. In Sherratt *et al.* (1995), the authors undertook a detailed investigation of that particular behaviour in the framework of

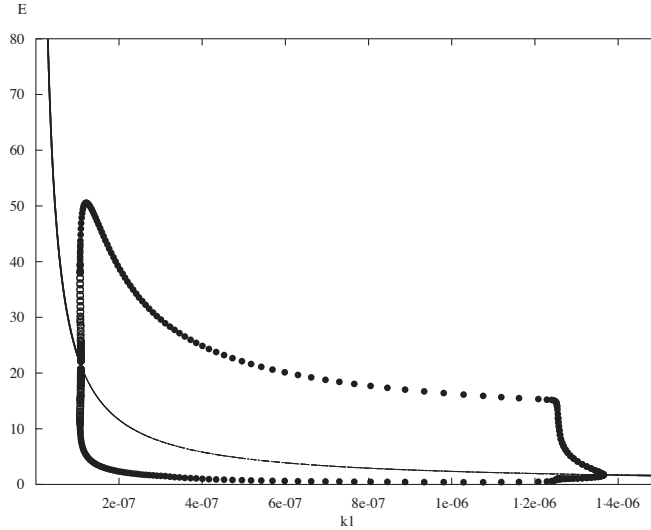


FIG. 12. Bifurcation diagram of TICL density  $E$  versus parameter  $k_1$ .

simplified reaction–diffusion equations of  $\lambda$ – $\omega$  type and were able to relate the appearance of these irregularities with periodic doubling and bifurcations to tori, which are well known routes to chaos. Concerns whether this kind of chaotic behaviour is a mathematical artifact rather than a biological reality have been raised in Sherratt *et al.* (1997) where theoretical arguments in favour of the latter were presented.

In the next section we will show that the particular limit cycle appearing in our simulations is a stable one which emerges through a Hopf bifurcation. In addition, the heterogeneities appearing in the long-time computations and the non-standard nature of the invading travelling waves will be related to the existence of the limit cycle.

## 5. Bifurcation analysis

In this section we undertake a numerical bifurcation analysis of the ODE system (27)–(29), that governs the kinetics of our model, first with respect to parameter  $k_1$  and then with respect to parameter  $p$ . The bifurcation diagrams presented here have been generated by the numerical continuation routine AUTO that is implemented within the XPP package (Ermentrout, 2002). AUTO provides implementation of numerical algorithms for tracking Hopf bifurcations and therefore establishing the existence of limit cycles.

Figure 12 shows part of the bifurcation diagram of TICL density  $E$  versus parameter  $k_1$ . In the case of our system AUTO was able to detect a (sub-critical) Hopf bifurcation at  $k_1 = 1.364 \times 10^{-6} \text{ day}^{-1} \text{ cells}^{-1} \text{ cm}$ . The solid dots represent the maximum and minimum values of the periodic solutions that emerge when  $k_1$  lies in a particular interval. Most of the limit cycles that emerge through this bifurcation, including the one that is generated for  $k_1 = 1.3 \times 10^{-7} \text{ day}^{-1} \text{ cells}^{-1} \text{ cm}$  (the value with which we have run the simulations in the previous sections), have been characterized by AUTO as stable. However, there is a region

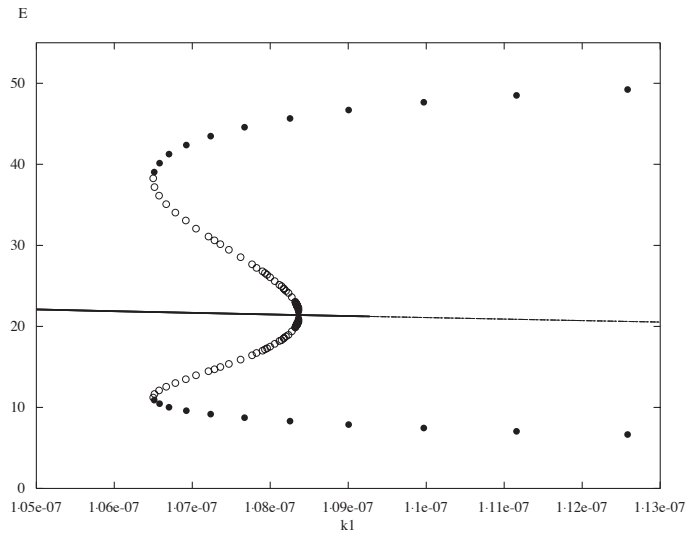


FIG. 13. Magnification of the left part of Fig. 12. The solid dots represent stable limit cycle solutions and the open circles represent unstable limit cycle solutions.

around  $k_1 = 1.08 \times 10^{-7} \text{ day}^{-1} \text{ cells}^{-1} \text{ cm}$  where unstable limit cycles exist. Figure 13 shows a detailed view of this part of the bifurcation diagram. As can be seen we have co-existence of stable and unstable limit cycles. Finally, it is worth mentioning that in the region of Figs 12 and 13 where  $k_1 < 1.06 \times 10^{-7} \text{ day}^{-1} \text{ cells}^{-1} \text{ cm}$ , no periodic solutions exist, and a stable spiral appears.

Next, we consider the bifurcations of the state variables with respect to  $p$ . The motivation for the choice of  $p$  as a control parameter lies in the heuristic consideration that by reducing the probability of tumour cells being killed by lymphocytes, travelling-wave-like solutions of more canonical nature should emerge and the special phase space structure related to the existence of the 3D attractor discussed in the previous section should alter.

Figure 14 show the bifurcation diagrams of the state variables  $E$ ,  $T$  and  $C$  with respect to parameter  $p$ . The ‘healthy’ steady state, which does not depend on  $p$ , is not included in these diagrams. The appearance of more steady states than the ‘tumour dormancy’ and ‘healthy’ ones for a particular range of  $p$  is revealed. The upper part of the bifurcation curve of the tumour cell density  $T$  represents the ‘tumour invasion’ steady states, which are stable. By solving numerically the ODE system, we have found that for  $p$  less than a critical value (approximately 0.9906) the limit cycle disappears and all the orbits that correspond to non-steady solutions converge to the ‘tumour invasion’ steady state. For  $p$  less than 0.96 the ‘tumour dormancy’ steady state disappears. We also carried out simulations of the PDE system (with and without chemotaxis) for values of  $p$  less than 0.9906. In this case the solution concerning  $T$  behaves like a standard travelling wave. Figure 15 depicts four snapshots in time of the tumour invasion that emerges by setting the parameter  $p$  equal to 0.99. According to these numerical observations the existence of the limit cycle in the phase space is highly relevant to the irregular nature of the invasive ‘wave’.

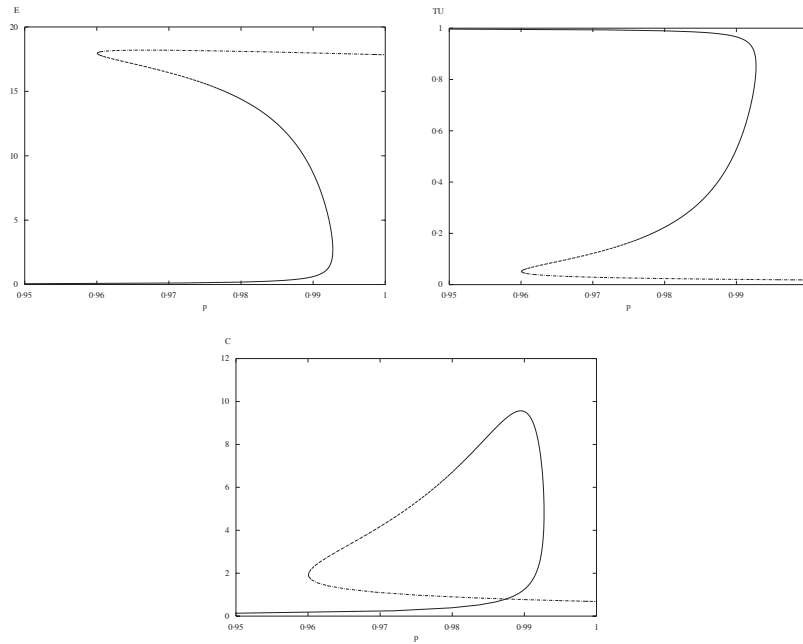


FIG. 14. Bifurcation diagrams of TICL density  $E$ , tumour cell density  $T$  and tumour cell–TICL complex density  $C$  versus the parameter  $p$ .

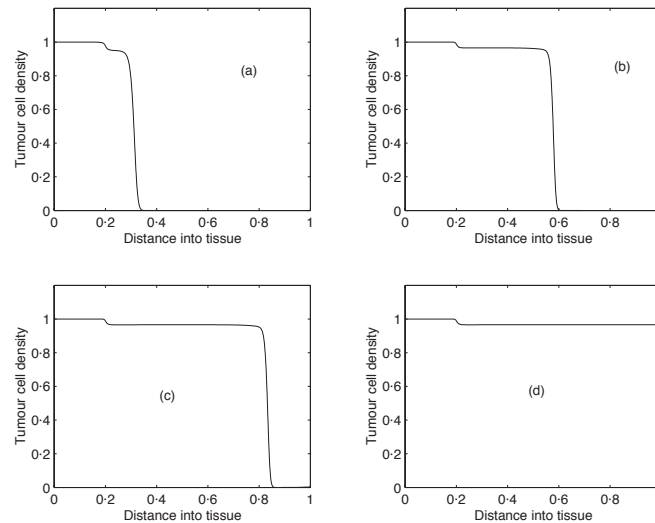


FIG. 15. ‘Travelling wave’ of tumour cell density  $T$  at times corresponding to 100, 400, 700 and 1000 days respectively. The parameter  $p$  has been set equal to 0.99.

We note that we also ran several spatial simulations (not shown here) with  $h(x) = 1, \forall x \in [0, 1]$  and although the solutions were different quantitatively (as expected) they display the same qualitative behaviour. Thus, the bounded irregular behaviour of the

solutions is not an outcome of the introduction of the Heaviside function, but as we have already indicated it is rather related to the coupling of the oscillatory ODE dynamics with diffusion. However, in the absence of the Heaviside function the source term leads to a homogeneous distribution of TICLs within the tumour in the first time step of the numerical integration, which is biologically unrealistic. Hence, the Heaviside function enables the simulations to display an infiltration of the tumour by TICLs only through the processes of diffusion and chemotaxis.

## 6. Radially symmetric solid tumour growth

In this section we solve numerically the system of equations (23), (25), and (26) in a radially symmetric three-dimensional setting. In particular, we seek solutions of the form  $E(r, t)$ ,  $T(r, t)$ , and  $C(r, t)$  where  $r$  is the radius in spherical polar coordinates. In this setting we are assuming that the growth of the solid tumour represents the early avascular phase observed in multicell spheroids. We assume that there is no necrotic core only viable, proliferating cells. We also study the case where chemotaxis is not present (i.e.  $\gamma = 0$ ). Rewriting the system in terms of spherical coordinates (assuming that all the partial derivatives of  $E$  and  $T$  with respect to the spherical polar angles  $\theta$  and  $\phi$  are equal to zero) we have

$$\frac{\partial E}{\partial t} = \frac{1}{r^2} \left[ \frac{\partial}{\partial r} \left( r^2 \frac{\partial E}{\partial r} \right) \right] + \sigma h(r) + \frac{\rho C}{\eta + T} - \sigma E - \mu ET + \epsilon C, \quad (31)$$

$$\frac{\partial T}{\partial t} = \frac{1}{r^2} \left[ \frac{\partial}{\partial r} \left( \omega r^2 \frac{\partial T}{\partial r} \right) \right] + \beta_1(1 - \beta_2 T)T - \phi ET + \lambda C, \quad (32)$$

$$\frac{\partial C}{\partial t} = \mu ET - \psi C. \quad (33)$$

The results of the numerical simulations are presented in Figs 16–18 which show cross sections through the spherical tumour. Figure 16 shows the spatial distribution of TICL density within the tissue at times corresponding to 100, 400, 700 and 1000 days respectively. The figures show a heterogeneous spatial distribution of TICL density throughout the tissue. Figure 17 shows the corresponding spatial distribution of tumour cell density within the tissue at times corresponding to 100, 400, 700 and 1000 days. The figures show a train of solitary-like waves invading the tissue and subsequently creating a spatially heterogeneous distribution of tumour cell density throughout. Figure 18 shows the corresponding spatial distribution of tumour cell-lymphocyte complexes within the tissue at times corresponding to 100, 400, 700 and 1000 days respectively.

## 7. Discussion and conclusions

In this paper we have examined a spatio-temporal mathematical model describing the growth of a solid tumour in the presence of an immune system response. In particular, we focused attention upon the interaction of tumour cells with a special sub-population of T-cells, so-called tumour-infiltrating cytotoxic lymphocytes (TICLs), in a relatively small, multicellular tumour, without central necrosis and at some stage prior to tumour-induced angiogenesis. At this early stage of solid tumour growth we investigated the situation

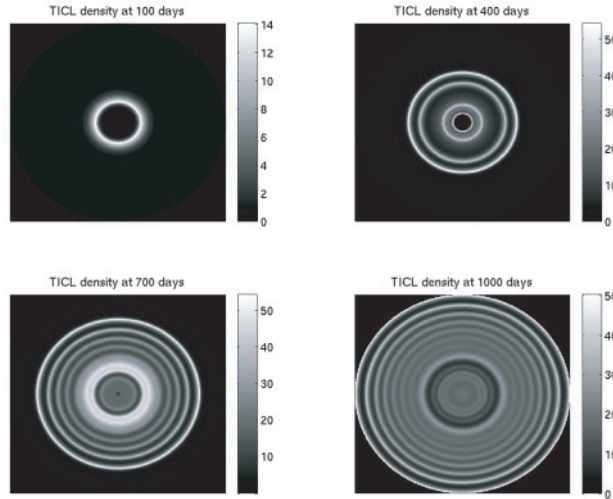


FIG. 16. Spatial distribution of TICL density within the tissue at times corresponding to 100, 400, 700 and 1000 days respectively.

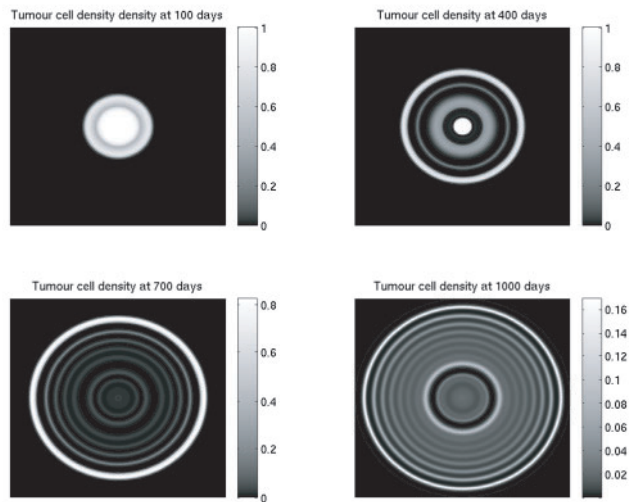


FIG. 17. Spatial distribution of tumour cell density within the tissue at times corresponding to 100, 400, 700 and 1000 days respectively.

whereby the immune cells and the tumour cells are in a state of dynamic equilibrium (cancer dormancy).

Our numerical and bifurcation analysis of the spatio-temporal model of cytotoxic T cell dynamics in cancer tissue supports the idea that the TICLs can play an important role in

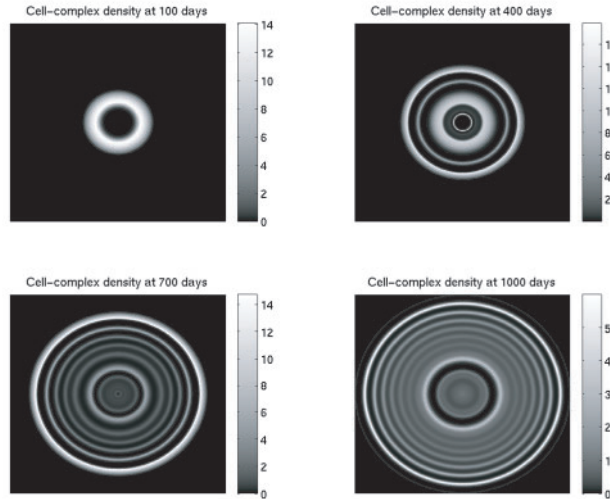


FIG. 18. Spatial distribution of tumour cell–TICL complex density within the tissue at times corresponding to 100, 400, 700 and 1000 days respectively.

the control of cancer dormancy. Moreover, the model allowed us to identify certain critical parameters of the process in which cancer cells are present in a tissue but do not clinically occur for a long period of time, but can begin to grow progressively at later date. Hence, our model could be potentially used to estimate the time interval between the primary treatment of an immunogenic tumour and tumour recurrence.

The T-lymphocytes were assumed to migrate into the growing solid tumour and interact with the tumour cells in such a way that lymphocyte–tumour cell complexes were formed. These complexes resulted in either the death of the tumour cells (the normal situation) or the inactivation (sometimes even the death) of the lymphocytes (Kuznetsov, 1979; Kuznetsov *et al.*, 1994). The migration of the TICLs was determined by a combination of random motility and chemotaxis in response to the presence of specialized chemoattractants (chemokines). The resulting system of four nonlinear partial differential equations (TICLs, tumour cells, complexes and chemokines) was analysed and numerical simulations were presented. The numerical simulations demonstrated the existence of dynamics that are quasi-stationary in time but heterogeneous in space. A subsequent linear stability analysis of the underlying (spatially homogeneous) ODE kinetics coupled with a numerical investigation of the ODE system revealed the existence of a stable limit cycle in the corresponding phase space. This was verified further when a bifurcation analysis was undertaken using the numerical continuation package XPPAUT.

We note that heterogeneous spatial patterning in an immune-system model has been found by Owen & Sherratt (1997, 1998, 1999) concerning macrophage interactions with tumour/mutant cells. In this case, however, the patterning was produced via an activator–inhibitor (Turing) mechanism by considering the mutant cells as the local activator and the chemical regulator as the long-range inhibitor. There are some significant differences between that work and the one presented here. The kinetics of the model presented in

Owen & Sherratt (1999) did not exhibit any Hopf bifurcation and, in the absence of a macrophage-based immunotherapy, the introduction of a small mutant cell density always caused the system to evolve to one of the two possible tumour invasion steady states it was able to predict. In our case, depending on the choice of parameters, the system kinetics may evolve to a tumour invasion steady state but they can also display an oscillatory behaviour with the tumour cell density bounded as a result of the cytotoxic activity of the TICLs.

Perhaps more appropriately, the evolution of the formal kinetics of our system appears to have some similarities with the evolution of the ODE kinetics of the ecological models presented in Sherratt *et al.* (1995). In both cases the global dynamics concerning the positive solutions consist of two unstable steady states and a stable limit cycle emerging through a Hopf bifurcation. However, some differences between the models exist with the most obvious of them being the different biological frameworks (ecology vs. immunology) and the difference in the dimensions of the corresponding phase spaces. We note that previous authors have pointed out the existence of similarities between the immune system response to immunogenic antigens and predator-prey ecological interactions (Nowak & May, 2000) (and more generally an ‘ecological competition’ between cancer cells and normal tissue cells: Gatenby, 1996, 1995) and that the mathematical particularities of our system could lead to entirely different spatio-temporal dynamics than those presented in Sherratt *et al.* (1995). This is to be investigated.

The numerical predictions of our model make it possible to comprehend the mechanisms involved in the appearance of spatio-temporal heterogeneities detected in solid tumours infiltrated by cytotoxic lymphocytes. These are described in numerous immunomorphological investigations (Berezhnaya *et al.*, 1986; Nesvetov & Zhdanov, 1981). However, in the material discussed in this paper, only some general problems associated with the mathematical theory of the interaction of TICLs with tumour cells have been examined. Future work mathematically will investigate whether or not spatio-temporal chaos is present.

We note that this model could be extended further. Specifically, an explicitly two dimensional (space) model could be investigated, enabling us to study the effect of asymmetry. Explicit interactions between the cancer cells and the host tissue could be incorporated into the basic kinetic model (Fig. 1). For example, Webb *et al.* (2002) proposed a mathematical model of a tumour cell ‘counter-attack’ against cytotoxic T-cells. The model consists of ordinary differential equations which represent the cross-linking of FasL and Fas. The authors consider the antagonistic interactions of two cell types: armed effector T-cells, and FasL positive tumour cells. The model is based upon the observation that certain types of human tumours can produce functional FasL and can induce the apoptotic killing of activated lymphocytes *in vitro*.

Recent model-fitting predicts that the life time of effector T-cells *in vivo* could be short (about several days) (Kuznetsov & Knott, 2001). Long-term maintenance of anticancer immunity after stopping immunotherapy could be improved if long-life immune memory cells could be activated during immunization. In particular, numerical modelling by Kuznetsov & Knott (2001) suggests that immune memory T-killer cells could be critical targets for immunization and vaccination strategies against solid tumours. Thus, an incorporation of the memory cells in our model could be helpful in better understanding cancer dormancy and cancer re-growth mechanisms and in optimizing the therapeutic strategy to reduce the risk of tumour relapse.

Finally, the familiar concept of a central necrotic core (and explicit oxygen distribution/uptake) could also be incorporated. It has been stated that the rate of macrophage and neutrophil accumulation in a spheroid depends on the density of tumour cells and is determined by a law analogous to that of Michaelis–Menten kinetics, while the accumulation of immune lymphocytes in a tumour is determined by the three-cell cooperation of lymphocytes, macrophages and tumour cells (Kuznetsov *et al.*, 1993). This data could provide further adaptations to our model, incorporating new cell types and increasing the realism of the system.

We hope that the results presented here (and the effects caused by the nonlinearity of the system) will make it possible for researchers and clinicians to have a better idea of the complicated and sometimes counter-intuitive outcome of processes occurring in immune-system interactions with tumour cells and thereby to develop more effective immunotherapy strategies and treatments for the control and possible elimination of cancers (Schirrmacher, 2001; Uhr & Marches, 2001; Demicheli, 2001). Our modelling and analysis offers the potential for quantitative analysis of mechanisms of tumour-cell–host-cell interactions and for the optimization of tumour immunotherapy and genetically engineered anti-tumour vaccines.

### Acknowledgments

AM gratefully acknowledges the generous financial support provided by Ms. Calliroe Lyras.

### REFERENCES

- ABBAS, A. K., LICHTMAN, A. H. & POBER, J. S. (2000) *Cellular and Molecular Immunology* 4th edn. Philadelphia, PA: Saunders.
- ADAM, J. A. (1993) The dynamics of growth-factor-modified immune response to cancer growth: One dimensional models. *Math. Comput. Modelling*, **17**, 83–106.
- ADAM, J. A. & BELLOMO, N. (eds) (1997) *A Survey of Models for Tumor-Immune System Dynamics*. Boston: Birkhäuser.
- ALSABTI, A. (1978) Tumour dormant state. *Tumour Res.*, **13**, 1–13.
- BAR-ELI, M. (1999) Role of interleukin-8 in tumor growth and metastasis of human melanoma. *Pathobiology*, **67**, 12–18.
- BEREZHNAJA, N. M., YAKIMOVICH, L. V., SEMENOVA KOBZAR, R. A., LYULKIN, V. D. & PAPIVETS, A. YU. (1986) The effect of interleukin-2 on proliferation of explants of malignant soft-tissue tumours in diffusion chambers. *Exp. Oncol.*, **8**, 39–42.
- BOHMAN, Y. V. (1976) *Metastases of Corpus Uterus Cancer*. Leningrad: Medicine.
- BRESLOW, N., CHAN, C. W., DHOM, G., DRURY, R. A., FRANKS, L. M., GELLEI, B., LEE, Y. S., LUNDBERG, S., SPARKE, B., STERNBY, N. H. & TULINIUS, H. (1977) Latent carcinoma of prostate at autopsy in seven areas. *Int. J. Cancer*, **20**, 680–688.
- BROCKER, E. B., ZWALDO, G., HOLZMANN, B., MACHER, E. & SORG, C. (1988) Inflammatory cell infiltrates in human melanoma at different stages of tumour progression. *Int. J. Cancer*, **41**, 562–567.
- BYRNE, H. M. & OWEN, M. R. (2001) Use of mathematical models to simulate and predict macrophage activity in diseased tissues. *The Macrophage*, 2nd edn. (B. Burke & C. E. Lewis, eds). Oxford: Oxford University Press.

- CAIRNS, C. M., GORDON, J. R., LI, F., BACA-ESTRADA, M. E., MOYANA, T. & XIANG, J. (2001) Lymphotaktin expression by engineered myeloma cells drives tumor regression: mediation by CD4+ and CD8+ T cells and neutrophils expressing XCR1 receptor. *J. Immunol.*, **167**, 57–65.
- CHAPLAIN, M. A. J., KUZNETSOV, V. A., JAMES, Z. H. & STEPANOVA, L. A. (1998) Spatio-temporal dynamics of the immune system response to cancer. *Mathematical Models in Medical and Health Sciences*. (M. A. Horn, G. Simonett & G. Webb, eds). Nashville, TN: Vanderbilt University Press, pp. 1–20.
- CLARK, W. H. (1991) Tumour progression and the nature of cancer. *Br. J. Cancer*, **64**, 631–644.
- CLARK, W. H., ELDER, D. E. & VANHORN, M. (1986) The biologic forms of malignant melanoma. *Human Pathol.*, **17**, 443–450.
- COWAN, D. S., HICKS, K. O. & WILSON, W. R. (1996) Multicellular membranes as an in vitro model for extravascular diffusion in tumours. *Br. J. Cancer Suppl.*, **27**, S28–S31.
- CROSS, M. C. & HOHENBERG, P. C. (1993) Pattern formation outside equilibrium. *Rev. Mod. Phys.*, **65**, 851–1112.
- DEMICHELI, R. (2001) Tumour dormancy: findings and hypotheses from clinical research on breast cancer. *Semin. Cancer Biol.*, **11**, 297–305.
- DEWEGER, R. A., WILBRINK, B., MOBERTS, R. M. P., MANS, D., OSKAM, R. & DEN OTTEN, W. (1987) Immune reactivity in SL2 lymphoma-bearing mice compared with SL2-immunized mice. *Cancer Immun. Immunotherapy*, **24**, 1191–1192.
- DRASDO, D. & HÖHME, S. (2003) Individual-based approaches to birth and death in avascular tumours. *Math. Comput. Modelling*, **37**, 1163–1175.
- DURAND, R. E. & SUTHERLAND, R. M. (1984) Growth and cellular characteristics of multicell spheroids. *Recent Results in Cancer Research*, **95**, 24–49.
- ERMENTROUT, G. B. (2002) *Simulating, Analyzing, and Animating Dynamical Systems: A Guide to XPPAUT for Researchers and Students* Software, Environments, and Tools, 14. SIAM.
- ERMENTROUT, G. B., CHEN, X. & CHEN, Z. (1997) Transition fronts and localized structures in bistable reaction–diffusion systems. *Physica D*, **108**, 147–167.
- FOLKMAN, J. (1985) How is blood-vessel growth regulated in normal and neoplastic tissue. *Proc. Am. Assoc. Cancer Res.*, **26**, 384–385.
- FORNI, G., PARMIANI, G., GUARINI, A. & FOA, R. (1994) Gene transfer in tumour therapy. *Annals Oncol.*, **5**, 789–794.
- FRIEDL, P., NOBLE, P. B. & ZANKER, K. S. (1995) T-Lymphocyte locomotion in a 3-dimensional collagen matrix—expression and function of cell-adhesion molecules. *J. Immunol.*, **154**, 4973–4985.
- GATENBY, R. A. (1995) Models of tumor-host interaction as competing populations: implications for tumor biology and treatment. *J. Theor. Biol.*, **176**, 447–455.
- GATENBY, R. A. (1996) Application of competition theory to tumour growth: implications for tumour biology and treatment. *Eur. J. Cancer*, **32A**, 722–726.
- AGUIRRE GHISO, J. A. (2002) Inhibition of FAK signaling activated by urokinase receptor induces dormancy in human carcinoma cells in vivo. *Oncogene*, **21**, 2513–2524.
- GIOVARELLI, M., CAPPELLO, P., FORNI, G., SALCEDO, T., MOORE, P. A., LEFLEUR, D. W., NARDELLI, B., CARLO, E. D., LOLLINI, P. L., RUBEN, S., ULLRICH, S., GAROTTA, G. & MUSIANI, P. (2000) Tumor rejection and immune memory elicited by locally released LEC chemokine are associated with an impressive recruitment of APCs, lymphocytes and granulocytes. *J. Immunol.*, **164**, 3200–3206.
- HOLMBERG, L. & BAUM, M. (1996) Work on your theories!. *Nature Med.*, **2**, 844–846.
- IOANNIDES, C. G. & WHITESIDE, T. L. (1993) T-cell recognition of human tumours—implications

- for molecular immunotherapy of cancer. *Clin. Immunol. Immunopath.*, **66**, 91–106.
- JAASKELAINEN, J., MAENPAA, A., PATARROYO, M., GAHMBERG, C. G., SOMERSALO, K., TARKKANEN, J., KALLIO, M. & TIMONEN, T. (1992) Migration of recombinant IL-2-activated T-cells and natural killer cells in the intercellular space of human H-2 glioma spheroids in vitro—a study on adhesion molecules involved. *J. Immunol.*, **149**, 260–268.
- KAWAKAMI, Y., NISHIMURA, M. I., RESTIFO, N. P., TOPALIAN, S. L., O'NEIL, B. H., SHILYANSKY, J., YANNELLI, J. R. & ROSENBERG, S. A. (1993) T-cell recognition of human-melanoma antigens. *J. Immunotherapy*, **14**, 88–93.
- KELLY, C. E., LEEK, R. D., BYRNE, H. M., COX, S. M., HARRIS, A. L. & LEWIS, C. E. (2002) Modelling macrophage infiltration into avascular tumours. *J. Theor. Med.*, **4**, 21–38.
- KOBAYASHI, R., OHTA, T. & HAYASE, Y. (1995) Self-organized pulse generator. *Physica D*, **84**, 162–170.
- KUZNETSOV, V. A. (1979) Dynamics of cellular immune anti-tumor reactions. I. Synthesis of a multi-level model. *Mathematical Methods in the Theory of Systems*. (V. D. Fedorov, ed.). Frunze: Kirghyz State University, pp. 57–71 (In Russian)
- KUZNETSOV, V. A. (1991) A mathematical model for the interaction between cytotoxic lymphocytes and tumor cells. Analysis of the growth, stabilization and regression of the B cell lymphoma in mice chimeric with respect to the major histocompatibility complex. *Biomed. Sci.*, **2**, 465–476.
- KUZNETSOV, V. A. (1992) *Dynamics of Immune Processes During Tumor Growth*. Moscow: Nauka, (In Russian)
- KUZNETSOV, V. A. & KNOTT, G. D. (2001) Modeling tumor regrowth and immunotherapy. *Math. Comput. Modelling*, **33**, 1275–1287.
- KUZNETSOV, V. A., MAKALKIN, I. A., TAYLOR, M. A. & PERELSON, A. S. (1994) Nonlinear dynamics of immunogenic tumours: parameter estimation and global bifurcation analysis. *Bull. Math. Biol.*, **56**, 295–321.
- KUZNETSOV, V. A. & PURI, R. K. (1999) Kinetic analysis of the high affinity forms of interleukin (IL)-13 receptors: suppression of IL-13 binding by IL-2 receptor  $\gamma$  chain. *Biophys. J.*, **77**, 154–172.
- KUZNETSOV, V. A. & STEPANOVA, L. A. (1992) Space-time waves and dissipative structures in a model of growth of tumours infiltrated by immune lymphocytes. *Lecture Notes of the ICB Seminars Biosystems*. (G. I. Marchuk & A. Werynski, eds). Warsaw, Poland: International Center for Biocybernetics, pp. 68–111.
- KUZNETSOV, V. A., ZHIVOGLYADOV, V. P. & STEPANOVA, L. A. (1993) Kinetic approach and estimation of the parameters of cellular interaction between the immune system and a tumour. *Arch. Immunol. Therap. Exp.*, **41**, 21–32.
- KWOK, C. S., COLE, S. E. & LIAO, S. K. (1988) Uptake kinetics of monoclonal antibodies by human malignant melanoma multicell spheroids. *Cancer Res.*, **48**, 1856–1863.
- KYLE, A. H., CHAN, C. T. & MINCHINTON, A. I. (1999) Characterization of three-dimensional tissue cultures using electrical impedance spectroscopy. *Biophys. J.*, **76**, 2640–2648.
- LEE, J., MORAN, J. P., FENTON, B. M., KOCH, C. J., FRELINGER, J. G., KENG, P. C. & LORD, E. M. (2000a) Alteration of tumour response to radiation by interleukin-2 gene transfer. *Br. J. Cancer*, **82**, 937–944.
- LEE, L. F., HELLENDALL, R. P., WANG, Y., HASKILLA, J. S., MUKAIDA, N., MATSUSHIMA, K. & TING, J. P. (2000b) IL-8 reduces tumorigenicity of human ovarian cancer *in vivo* due to neutrophil infiltration. *J. Immunol.*, **164**, 2769–2775.
- LEFEVER, R. & ERNEUX, T. (1984) On the growth of cellular tissues under constant and fluctuating environmental conditions. *Nonlinear Electrodynamics in Biological Systems*. (W. Ross & A.

- Lawrence, eds). New York: Plenum, pp. 287–305.
- LOEFFLER, D., HEPPNER, G. & LORD, E. (1988) Influence of hypoxia on T lymphocytes in solid tumours. *Proc. Am. Assoc. Cancer Res.*, **29**, 378.
- LOEFFLER, D. & RATNER, S. (1989) In vivo localization of lymphocytes labeled with low concentrations of HOECHST-33342. *J. Immunol. Meth.*, **119**, 95–101.
- LORD, E. M. & BURKHARDT, G. (1984) Assessment of in situ host immunity to syngeneic tumours utilizing the multicellular spheroid model. *Cell. Immunol.*, **85**, 340–350.
- LORD, E. M. & NARDELLA, G. (1980) The multicellular tumour spheroid model. 2. characterization of the preliminary allograft response in unsensitized mice. *Transplantation*, **29**, 119–124.
- MACSWEEN, R. N. M. & WHALEY, K. (eds) (1992) *Muir's Textbook of Pathology* 13th edn. London: Arnold.
- MARUŠIĆ, M., BAJZER, Ž., VUK-PAVLOVIĆ, S. & FREYER, J. P. (1994a) Analysis of the growth of multicellular tumour spheroids by mathematical models. *Cell Prolif.*, **27**, 73–94.
- MARUŠIĆ, M., BAJZER, Ž., VUK-PAVLOVIĆ, S. & FREYER, J. P. (1994b) Tumour growth *in vivo* and as multicellular spheroids compared by mathematical models. *Bull. Math. Biol.*, **56**, 617–631.
- MERKIN, J. H. & SADIQ, M. A. (1996) The propagation of travelling waves in an open cubic autocatalytic chemical system. *IMA J. Appl. Math.*, **57**, 273–309.
- MURPHY, C. & NEWSHOLME, P. (1999) Macrophage-mediated lysis of a beta-cell line, tumour necrosis factor-alpha release from bacillus Calmette–Guerin (BCG)-activated murine macrophages and interleukin-8 release from human monocytes are dependent on extracellular glutamine concentration and glutamine metabolism. *Clin. Sci.*, **96**, 89–97.
- NAUMOV, G. N., MACDONALD, I. C., WEINMEISTER, P. M., KERKVLIT, N., NADKARNI, K. V., WILSON, S. M., MORRIS, V. L., GROOM, A. C. & CHAMBERS, A. F. (2002) Persistence of solitary mammary carcinoma cells in a secondary site: a possible contributor to dormancy. *Cancer Res.*, **62**, 2162–2168.
- NESVETOV, A. M. & ZHDANOV, A. S. (1981) Relationship of the morphology of the immune response and the histological structure of tumours in stomach cancer patients. *Voprosy Onkologii*, **27**, 25–31.
- NOMIYAMA, H., HIESHIMA, K., NAKAYAMA, T., SAKAGUCHI, T., FUJISAWA, R., TANASE, S., NISHIURA, H., MATSUNO, K., TAKAMORI, H., TABIRA, Y., YAMAMOTO, T., MIURA, R. & YOSHIE, O. (2001) Human CC chemokine liver-expressed chemokine/CCL16 is a functional ligand for CCR1, CCR2 and CCR5, and constitutively expressed by hepatocytes. *Int. Immunol.*, **13**, 1021–1029.
- NOWAK, M. A. & MAY, R. M. (2000) *Virus Dynamics: Mathematical Principles of Immunology and Virology*. Oxford: Oxford University Press.
- O'CONNELL, J., BENNETT, M. W., O'SULLIVAN, G. C., COLLINS, J. K. & SHANAHAN, F. (1999) The Fas counterattack: cancer as a site of immune privilege. *Immunol. Today*, **20**, 46–50.
- OWEN, M. R. & SHERRATT, J. A. (1997) Pattern formation and spatio-temporal irregularity in a model for macrophage-tumour interactions. *J. Theor. Biol.*, **189**, 63–80.
- OWEN, M. R. & SHERRATT, J. A. (1998) Modelling the macrophage invasion of tumours: Effects on growth and composition. *IMA J. Math. Appl. Med. Biol.*, **15**, 165–185.
- OWEN, M. R. & SHERRATT, J. A. (1999) Mathematical modelling of macrophage dynamics in tumours. *Math. Models Meth. Appl. Sci.*, **9**, 513–539.
- PREHN, R. T. (1994) Stimulatory effects of immune reactions upon the growths of untransplanted tumours. *Cancer Res.*, **54**, 908–914.
- PRIGOGINE, I. & LEFEVER, R. (1980) Stability problems in cancer growth and nucleation. *Comp. Biochem. Physiol.*, **67**, 389–393.

- PURI, R. K. & SIEGEL, J. P. (1993) Interleukin-4 and cancer therapy. *Cancer Invest.*, **11**, 473–486.
- RATNER, S. & HEPPNER, G. H. (1986) Mechanisms of lymphocyte traffic in neoplasia. *Anticancer Res.*, **6**, 475–482.
- REISENBERGER, K., EGARTER, C., VOGL, S., STERNBERGER, B., KISS, H. & HUSSLEIN, P. (1996) The transfer of interleukin-8 across the human placenta perfused in vitro. *Obstet Gynecol.*, **87**, 613–616.
- RETSKY, M. W., WARDWELL, R. H., SWARTZENDRUBER, D. E. & HEADLEY, D. L. (1987) Prospective computerized simulation of breast-cancer—comparison of computer-predictions with 9 sets of biological and clinical data. *Cancer Res.*, **47**, 4982–4987.
- ROTHSTEIN, T. L., MAGE, M. G., MOND, J. & MCHUGH, L. L. (1978) Guinea pig antiserum to mouse cytotoxic T-lymphocytes and their precursor. *J. Immunol.*, **120**, 209–215.
- SATYAMOORTHY, K., LI, G., VAIDYA, B., KALABIS, J. & HERLYN, M. (2002) Insulin-like growth factor-I-induced migration of melanoma cells is mediated by interleukin-8 induction. *Cell Growth Differ.*, **13**, 87–93.
- SCHIRRMACHER, V. (2001) T-cell immunity in the induction and maintenance of a tumour dormant state. *Semin. Cancer Biol.*, **11**, 285–295.
- SCHWARTZENTRUBER, D. J., TOPALIAN, S. L., MANCINI, M. & ROSENBERG, S. A. (1991) Specific release of granulocyte-macrophage colony-stimulating factor, tumour necrosis factor- $\alpha$  and IFN- $\gamma$  by human tumour-infiltrating lymphocytes after autologous tumour stimulation. *J. Immunol.*, **146**, 3674–3681.
- SHERRATT, J. A., EAGAN, B. T. & LEWIS, M. A. (1997) Oscillations and chaos behind predator-prey invasion: mathematical artifact or ecological reality?. *Phil. Trans. R. Soc. Lond. B*, **352**, 21–38.
- SHERRATT, J. A., LEWIS, M. A. & FOWLER, A. C. (1995) Ecological chaos in the wake of invasion. *Proc. Natl Acad. Sci. USA*, **92**, 2524–2528.
- SHERRATT, J. A., PERUMPANANI, A. J. & OWEN, M. R. (1999) Pattern formation in cancer. *On Growth and Form: Spatio-temporal Pattern Formation in Biology*. (M. A. J. Chaplain, G. D. Singh & J. C. McLachlan, eds). New York: Wiley.
- SIU, H., VITETTA, E. S., MAY, R. D. & UHR, J. W. (1986) Tumour dormancy. regression of BCL tumour and induction of a dormant tumour state in mice chimeric at the major histocompatibility complex. *J. Immunol.*, **137**, 1376–1382.
- SORDAT, B., MACDONALD, H. R. & LEES, R. K. (1980) The multicellular spheroid as a model tumour allograft. 3. morphological and kinetic analysis of spheroid infiltration and destruction. *Transplantation*, **29**, 103–112.
- SOZZANI, S., LUINI, W., MOLINO, M., JILEK, P., BOTTAZZI, B. & CERLETTI, C. (1991) The signal transduction pathway involved in the migration induced by a monocyte chemotactic cytokine. *J. Immunol.*, **147**, 2215–2221.
- SUTHERLAND, R. M. (1988) Cell and environment interactions in tumor microregions: the multicell spheroid model. *Science*, **240**, 177–184.
- SUZUKI, Y., LIU, C. M., CHEN, L. P., BENNATHAN, D. & WHEELLOCK, E. F. (1987) Immune regulation of the L5178Y murine tumour dormant state. 2. interferon gamma requires tumour necrosis factor to restrain tumour cell growth in peritoneal cell cultures from tumour dormant mice. *J. Immunol.*, **139**, 3146–3152.
- UDAGAWA, T., FERNANDEZ, A., ACHILLES, E. G., FOLKMAN, J. & D'AMATO, R. J. (2002) Persistence of microscopic human cancers in mice: alterations in the angiogenic balance accompanies loss of tumor dormancy. *FASEB J.*, **16**, 1361–1370.
- UHR, J. W. & MARCHES, R. (2001) Dormancy in a model of murine B cell lymphoma. *Semin. Cancer Biol.*, **11**, 277–283.

- UHR, J. W., TUCKER, T., MAY, R. D., SIU, H. & VITETTA, E. S. (1991) Cancer dormancy: studies of the murine BCL lymphoma. *Cancer Res. (Suppl.)*, **51**, 5045s–5053s.
- WEBB, S. D., SHERRATT, J. A. & FISH, R. G. (2002) Cells behaving badly: a theoretical model for the Fas/FasL system in tumour immunology. *Math. Biosci.*, **179**, 113–129.
- WHEELOCK, E. F., WEINHOLD, K. J. & LEVICH, J. (1981) The tumour dormant state. *Adv. Cancer Res.*, **34**, 107–140.
- WILSON, K. M. & LORD, E. M. (1987) Specific (EMT6) and non-specific (WEHI-164) cytolytic activity by host cells infiltrating tumour spheroids. *Br. J. Cancer*, **55**, 141–146.